Scientific Reports

https://doi.org/10.1038/s41598-026-46404-1

Article in Press

Energy efficient thermal and hydraulic performance analysis of a serpentine liquid cooled lithium ion battery pack for electric vehicles

Received: 3 January 2026

Accepted: 25 March 2026

Published online: 03 April 2026

Cite this article as: Dagnaw E.S., Aga A.G. & Sufe G. Energy efficient thermal and hydraulic performance analysis of a serpentine liquid cooled lithium ion battery pack for electric vehicles. *Sci Rep* (2026). https://doi.org/10.1038/s41598-026-46404-1

Eshetu Setegn Dagnaw, Amanuel Gebisa Aga & Gadisa Sufe

Energy Efficient Thermal and Hydraulic Performance Analysis of a Serpentine Liquid Cooled Lithium Ion Battery Pack for Electric Vehicles

Eshetu Setegn Dagnaw[1], Amanuel Gebisa Aga[2], Gadisa Sufe[3*]

[1] Department of Motor Vehicle Engineering, College of Engineering, Ethiopian Defence University, P.O. Box 1041, Bishoftu, Ethiopia
[2] Department of Mechanical Engineering, Adama Science and Technology University, Adama, Ethiopia
[3] Faculty of Mechanical Engineering, Wrocław University of Science and Technology, Wrocław, 50-370, Poland

Corresponding Author: Amanuel Gebisa Aga (kumynnh.coe@etdu.edu.et)

Abstract

Efficient thermal regulation of lithium ion battery packs is essential for electric vehicle safety, durability, and energy efficiency, particularly under high power operation. This study numerically investigates the thermal and hydraulic performance of a serpentine liquid cooled aluminum cold plate integrated into a 288-cell prismatic battery pack. A three-dimensional conjugate heat transfer model was developed in ANSYS Fluent to resolve coupled heat generation, conduction, and coolant flow behavior under a total thermal load of 2880 W. At a coolant flow rate of 9.84 L per minute, the proposed design maintained cell temperatures between 298 K and 308 K, with a maximum temperature of 315.3 K and temperature non-uniformity of plus or minus 4 °C. The pressure drop across the cooling channels was 15 kPa, while pumping losses accounted for only 4.2 % of the total thermal energy removed. Compared with a conventional parallel flow cold plate, the serpentine configuration reduced peak temperature by 2.7 % and improved temperature uniformity by 20 %. The novelty of this work lies in the integrated quantitative evaluation of thermal performance, hydraulic penalty, and energy efficiency at full pack scale, providing design guidance for compact and energy conscious battery thermal management system

Keywords: Lithium ion battery thermal management; Serpentine liquid cooling; Aluminum cold plate; Electric vehicle battery pack; Thermal fluid numerical modeling

1. Introduction

The global transition from internal combustion engine dominated transportation toward electric mobility has intensified in recent years, driven by the dual imperatives of reducing greenhouse gas emissions and improving energy efficiency within the transportation sector [1,2]. Electric vehicles have emerged as a viable and necessary pathway toward sustainable mobility, particularly as governments impose increasingly stringent emission regulations and societies recognize the long-term environmental and economic consequences of continued fossil fuel dependence [3,4]. Despite substantial advances in battery chemistry, power electronics, and vehicle integration, the performance and reliability of electric vehicles remain fundamentally constrained by the thermal behavior of lithium-ion battery systems. As a result, battery thermal management has become a decisive factor influencing vehicle safety, durability, energy efficiency, and consumer acceptance [5,6].

Lithium-ion batteries generate heat as an inherent consequence of electrochemical reactions, internal resistance, and entropy changes during charge and discharge cycles [7].Several modeling approaches have been proposed in the literature to describe heat generation in lithium-ion batteries, ranging from simplified lumped thermal models to fully coupled electrochemical–thermal formulations. Recent studies have shown that total heat generation consists primarily of irreversible Joule heating due to internal resistance and

reversible entropic heat associated with electrochemical reactions, both of which depend on current, state of charge, and temperature [8,9] Advanced electrochemical–thermal models resolve these contributions dynamically and provide high fidelity predictions under transient operating conditions, such as fast charging and aggressive drive cycles.

However, system-level thermal management studies frequently adopt simplified heat generation models in which the battery is represented by an equivalent constant or averaged volumetric heat source. Such approaches have been demonstrated to provide reliable predictions of temperature distribution and cooling effectiveness when the primary objective is the evaluation of cooling architecture and thermal–hydraulic performance rather than detailed electrochemical behavior. Recent investigations confirm that for steady-state or quasi-steady operating conditions, constant heat generation assumptions yield results that are consistent with more complex models while significantly reducing computational cost [10,11].

Heat generation intensifies under conditions of high current operation, fast charging, regenerative braking, and elevated ambient temperatures. If not properly managed, excessive heat accumulation leads to non-uniform temperature distributions within individual cells and across the battery pack [12,13]. Such thermal non-uniformity accelerates degradation mechanisms, including active material loss, electrolyte decomposition, and lithium plating, ultimately reducing battery capacity, cycle life, and energy efficiency. More critically, localized hot spots can initiate thermal runaway, posing significant safety risks [14,15]. These challenges are particularly acute in light-duty electric vehicles, where compact packaging, limited cooling space, weight constraints, and variable driving conditions restrict the use of large or energy-intensive thermal management systems. Consequently, achieving precise and uniform thermal regulation under realistic operational conditions remains a persistent challenge that has not been fully resolved by existing technologies [16,17].

State-of-the-art battery thermal management systems can be broadly classified into passive, active, and hybrid configurations. Passive systems rely on natural convection, conduction, or latent heat absorption and are attractive due to their simplicity, low cost, zero parasitic power consumption, and minimal system complexity [18,19]. However, their cooling capacity is inherently limited, and they struggle to maintain acceptable temperature levels under high thermal loads associated with fast charging and aggressive driving. Active systems, including forced air and liquid cooling, offer significantly higher heat removal capability but introduce additional complexity, increased mass, high manufacturing cost, and continuous energy consumption [20,21]. Although liquid cooling systems generally perform better than air-based solutions, many existing designs suffer from non-uniform coolant distribution, inefficient heat transfer at the cell level, excessive pressure drop, and suboptimal integration with battery modules. Furthermore, several studies have focused on simplified geometries, steady-state conditions, or component-level analyses, limiting their applicability to full-scale battery packs operating under transient thermal loads [22,23].

Recent research efforts have sought to overcome the limitations of conventional cooling strategies through hybrid approaches that integrate passive and active mechanisms, advanced cold-plate architectures, and enhanced coolants. Two prominent themes in recent work involve the development of complex channel geometries, such as serpentine, U-shaped, and microchannel configurations, and the use of nanofluid coolants with enhanced thermal properties [24–26]. While these innovations show promise, important limitations remain. Many studies on advanced channel designs emphasize peak temperature reduction without adequately quantifying spatial temperature uniformity or evaluating the hydraulic penalties, such as increased pressure drop and pumping power [27,28]. Others focus on narrow ranges of operating conditions, ignoring variations in battery heat generation due to load cycling, ambient fluctuations, or state-of-charge dependent behavior. Furthermore, comparisons between advanced designs and baseline systems are often incomplete, lacking rigorous benchmarking under standardized performance metrics that include both thermal and hydraulic criteria [29,30].

The application of nanofluid coolants, such as those incorporating aluminum oxide or other particulate additives, has been reported to improve effective thermal conductivity and heat transfer rates. However, recent studies point out that the long-term stability, particle agglomeration, erosion effects, and compatibility with pump and channel materials remain underexplored [31]. Many numerical investigations assume idealized nanofluid behavior without accounting for sedimentation, viscosity changes, or real-world degradation over extended operational periods. Similarly, empirical validation of nanofluid performance in full-scale battery packs under transient conditions is scarce, limiting confidence in the scalability of these approaches [1,32]. Hybrid thermal management systems, which combine passive elements with liquid cooling or phase change materials, have shown improved performance in specific scenarios. Yet, their control strategies, energy consumption profiles, and response to dynamic thermal loads require deeper investigation to establish robust design guidelines [33].

Liquid-cooled cold-plate systems represent a promising yet still evolving solution for battery thermal management. Their effectiveness depends strongly on material selection, internal channel topology, flow distribution, and thermal coupling with battery cells [34]. Aluminum has emerged as a favorable cold-plate material due to its high thermal conductivity, low density, corrosion resistance, and compatibility with scalable manufacturing techniques. Serpentine flow channels offer extended flow paths and increased surface contact area, potentially enhancing heat extraction and enabling better control over temperature distribution [35,36]. However, the extended flow length and associated pressure drop inherent to serpentine designs can compromise coolant uniformity and raise pumping power requirements. Existing studies often evaluate serpentine configurations in isolation or compare them with simpler channel designs without systematically addressing these coupled thermal–hydraulic trade-offs at the pack level or under transient operating conditions [37–39].To focus on thermal–hydraulic optimization of the cooling architecture, the electrochemical heat generation is represented using an equivalent constant heat source, an approach commonly adopted in system-level battery thermal management studies.

Despite extensive research on liquid cooled battery thermal management systems, significant limitations persist at the pack scale. Most prior investigations concentrate on cell level or simplified module configurations and primarily report peak temperature reduction as the main performance indicator. Hydraulic resistance, pumping power, and temperature uniformity are often treated separately or omitted altogether. In addition, comparative assessments between serpentine and parallel cooling architectures are frequently conducted under non-identical geometric envelopes and heat generation conditions, which reduces the reliability and industrial relevance of the conclusions. A systematically benchmarked framework that integrates thermal and hydraulic performance at full pack scale therefore remains necessary.

This study addresses these gaps through a three-dimensional conjugate thermal fluid analysis of a 288-cell prismatic lithium ion battery pack equipped with aluminum serpentine cold plates under transient operating conditions. Unlike conventional approaches that emphasize temperature magnitude alone, the present work integrates peak temperature, spatial temperature uniformity, pressure drop, and pumping energy within a unified quantitative framework. By explicitly coupling thermal behavior with hydraulic and energy penalties, the analysis captures realistic engineering tradeoffs that govern practical battery pack design.

The primary novelty of this research lies in four aspects. First, it provides full pack scale simulation rather than isolated cell or simplified module analysis, thereby improving industrial representativeness. Second, it establishes measurable relationships between coolant flow rate, pressure drop, pumping energy, and temperature uniformity, enabling objective design optimization. Third, it directly benchmarks serpentine and parallel flow architectures under identical boundary conditions, geometric constraints, and heat generation rates, ensuring consistent and fair comparison. Fourth, it introduces explicit

energy accounting to evaluate whether thermal improvements justify the associated hydraulic cost.

From an engineering perspective, the findings deliver actionable design guidance for compact and manufacturable battery thermal management systems in electric vehicles. By identifying balanced operating regions that minimize peak temperature and thermal gradients without imposing excessive pumping energy, the study provides a practical pathway toward safer operation, improved durability, and enhanced overall battery performance.

The remainder of this article is organized as follows. Section 2 presents the methodology, including geometric modeling, numerical framework, governing equations, boundary conditions, and mesh convergence studies. Section 3 discusses results, focusing on temperature distribution, coolant flow optimization, comparative channel performance, and thermal-hydraulic trade-offs. Section 4 presents conclusions, emphasizing quantitative design guidelines and industrial applications.

2. Methodology

This study employs a comprehensive computational and analytical methodology to design, analyze, and evaluate a liquid-based battery thermal management system for a large-format lithium-ion battery pack intended for electric vehicle applications. The methodology is structured to ensure scientific rigor, physical consistency, and full reproducibility. By integrating detailed geometric modeling, advanced thermal–fluid simulations, and analytical heat transfer formulations, the approach captures the coupled interaction between internal battery heat generation and external liquid cooling under realistic operating conditions. Particular emphasis is placed on temperature uniformity, thermal safety margins, and energy efficiency, which are critical performance metrics for modern electric vehicles

2.1. Research Design and Framework

The present study adopts a simulation driven methodology supported by analytical thermal modeling to investigate the thermal behavior of an electric vehicle battery pack. A fully three-dimensional numerical model of the battery pack and liquid cooling system was developed to closely represent the physical configuration of a real-world electric vehicle application. The modeling framework integrates continuum scale conservation equations governing fluid flow and heat transfer with a discrete nodal thermal representation at the cell and module levels. This hybrid strategy enables simultaneous resolution of local temperature variations within individual cells and global thermal trends across the complete battery pack, providing a comprehensive assessment of thermal performance.

The computational domain corresponds to a full-scale battery pack with external dimensions of approximately 1860 mm × 1400 mm × 300 mm, consistent with the selected vehicle platform, the Volkswagen ID.4. The battery system comprises 288 large format prismatic lithium ion cells arranged into 12 modules, each containing 24 cells, in accordance with the reference vehicle architecture. An aluminum cold plate is located beneath the battery modules to facilitate effective heat removal through direct conductive contact. Internal serpentine coolant channels are explicitly modeled within the cold plate geometry to capture realistic coolant flow behavior. All geometric features, including cell dimensions, cooling plate thickness, channel configuration, and flow passages, were designed in SolidWorks and directly imported into the CFD solver. This procedure ensures geometric consistency between the physical design and the numerical model, thereby enhancing the practical relevance and scalability of the simulation for electric vehicle battery thermal management applications.

The simulations were performed under steady state operating conditions representative of typical battery discharge scenarios encountered during normal vehicle operation. Although transient thermal effects play an important role under real driving cycles, steady state analysis provides a reliable basis for evaluating baseline thermal characteristics, identifying potential hot spots, and assessing the inherent effectiveness of the cooling architecture. Moreover, this methodological approach reflects standard industrial design

and evaluation practices in battery thermal management development, further strengthening the applicability of the findings.

To ensure numerical stability, computational efficiency, and clarity in system level thermal hydraulic analysis, the numerical model is formulated based on the following assumptions. First, battery cells are considered thermally homogeneous, and internal temperature gradients within individual cells are neglected. Second, heat generation within each cell is modeled as a constant and uniform volumetric heat source, representing average heat generation during steady high load discharge. Third, electrochemical reactions are not explicitly resolved, and their thermal effects are incorporated through the equivalent heat source formulation. Fourth, material properties of all solid components and the coolant are assumed to be constant and independent of temperature. Fifth, radiative heat transfer between battery surfaces and the surroundings is neglected due to its relatively minor contribution compared to conduction and convection. Sixth, coolant flow is assumed to be incompressible, and gravitational effects are ignored. Finally, perfect thermal contact is assumed between the battery cells and the aluminum cooling plate, with no interfacial contact resistance.

These assumptions are consistent with widely accepted practices in system level battery thermal management studies and are considered appropriate for evaluating the cooling architecture performance under steady state operating conditions.

2.2. Materials, Data, and Tools

The battery system examined in this study comprises a 288-cell prismatic lithium ion battery pack organized into 12 modules, closely reflecting the architecture of a commercially deployed electric vehicle platform. This configuration preserves realistic geometric proportions, electrical capacity, and thermal loading characteristics representative of large-scale automotive applications. The Volkswagen ID.4 is selected as the reference vehicle, as its battery pack specifications provide a credible and well documented basis for numerical modeling, as summarized in Table 1. The pack is mounted beneath the vehicle floor between the front and rear axles, a layout that imposes stringent constraints on cooling system thickness, mass, and available packaging volume.

The battery pack consists of large format prismatic lithium ion cells representative of automotive grade chemistries, particularly NMC based systems that are widely adopted in current electric vehicles. In the present work, cell level electrochemical parameters are not experimentally characterized. Instead, effective thermophysical properties are adopted from established literature to capture the average thermal behavior under normal operating conditions. Electrochemical aging and degradation mechanisms are not explicitly modeled. Nevertheless, the influence of thermal exposure and temperature non-uniformity, which are widely recognized as key factors accelerating battery degradation, is directly addressed through the evaluation and optimization of the thermal management strategy.

Table 1: VW ID.4 Vehicle Specifications

Specification	Value
Gross Vehicle Weight Rating (GVWR)	~2,750 kg
Curb Weight	1,928–2,224 kg
Range	442-531 km
Overall Length	4,584 mm
Width	1,852 mm
Height	1,636 mm
Wheelbase	2,766 mm
Ground Clearance	~208 mm
Drive Options	RWD or AWD
Top Speed	160 km/h

Energy Consumption	15–20 kWh/100 km

Geometric modeling of the battery system was performed in SolidWorks, where individual cells, modules, structural components, and coolant channels were explicitly defined. This level of geometric detail enables accurate representation of conduction paths, contact surfaces, and fluid flow regions, which are critical for realistic thermal fluid simulations. The coolant used in the simulations is a 1:1 ethylene glycol water mixture, chosen for its favorable combination of thermal conductivity, specific heat capacity, and freeze protection, consistent with common automotive applications. Material properties for both the coolant and solid components were defined uniformly to ensure numerical stability and physical realism. Ambient boundary conditions were selected to represent the climatic conditions of Addis Ababa, capturing moderate operating temperatures typical of the region.

Ambient boundary conditions were selected to represent the climatic conditions of Addis Ababa. An ambient temperature of 298 K (25 °C) was applied to all external battery pack surfaces exposed to the environment. Natural convective heat transfer to the surroundings was modeled using a convective heat transfer coefficient of 5 $W/m^2 \cdot K$, consistent with typical underbody vehicle conditions and values reported in prior battery thermal management studies.

Table 2: VW ID.4 Battery Specifications

Specification	**Value**
Battery Type	Lithium-Ion
Battery Cell Type	Prismatic cell
Battery Pack Capacity	77 kWh
Battery Weight	493 kg
Number of Cells	288 cells (12 modules)
Battery Position	Floor-mounted, between axles
Battery Dimensions (L × W × H)	1,860 mm × 1,400 mm × 300 mm
Cooling Requirements	Advanced cooling system
Nominal voltages	403V
Nominal capacity	160AH

Thermal–fluid simulations were conducted using ANSYS Fluent, which solved the governing equations for incompressible flow and heat transfer within both solid and fluid domains. Post-processing in ANSYS Fluent allowed detailed visualization of temperature contours, velocity vectors, and heat flux distributions, facilitating analysis of both local and pack-level thermal behavior. The key specifications of the Volkswagen ID.4 battery pack, including battery type, cell configuration, total capacity, and module arrangement, are summarized in Table 2. Integrating realistic geometric, thermal, and material data with accurate environmental conditions ensures that the simulation outcomes closely represent practical operating scenarios, providing a robust foundation for evaluating battery thermal management performance.

2.3. Procedures and Simulation Protocol

The simulation procedure was executed in a structured and sequential manner to ensure clarity and reproducibility. Initially, a complete three-dimensional CAD model of the battery pack and integrated liquid cooling plate was developed. The cooling plate was positioned beneath the battery modules to promote efficient heat extraction through conduction from the cell bases and subsequent convection into the circulating coolant. Internal flow channels were designed to distribute coolant uniformly across the cooling plate surface, thereby minimizing temperature gradients between adjacent cells and modules.

The CAD geometry was then imported into ANSYS Fluent for meshing and simulation setup. A hybrid meshing strategy was employed to balance accuracy and computational efficiency. Hexahedral elements were used in geometrically regular regions to reduce numerical diffusion, while tetrahedral elements were applied in complex regions where geometric flexibility was required. Inflation layers were introduced near solid–fluid interfaces to accurately resolve velocity and thermal boundary layers, which play a critical role in convective heat transfer.

Mesh quality was rigorously controlled to ensure reliable numerical results. Skewness was maintained below 0.5, aspect ratios were kept within acceptable limits near walls, and overall element quality exceeded recommended thresholds. Following meshing, boundary conditions, material properties, and solver settings were defined. Simulations were performed using a steady-state solver, and approximately 500 iterations were executed for each case to ensure convergence of residuals and stabilization of key solution variables. Convergence was assessed based on residual reduction and monitoring of temperature and pressure values at critical locations within the battery pack.

2.4. Mathematical Models and Governing Equation

The thermal and fluid behavior of the battery thermal management system is governed by the fundamental conservation laws of mass, momentum, and energy for incompressible flow. Mass conservation of the coolant is enforced through the continuity equation, which ensures that the mass flow rate remains constant throughout the cooling channels. Momentum conservation is described by the Navier–Stokes equations, accounting for pressure forces and viscous effects within the flowing coolant. Under steady state conditions and in the absence of body forces, these equations are simplified while still capturing the dominant physical behavior relevant to liquid cooling systems used in battery applications.

Based on the classical continuity, momentum, and energy equations, a mathematical model was developed to describe heat generation within the battery cells and its subsequent propagation through the battery pack. Numerical simulation tools such as ANSYS enable engineers to predict thermal behavior and evaluate operating conditions that would be difficult or expensive to reproduce experimentally. In this sense, the model functions as a virtual testing environment, allowing designers to assess battery thermal response under demanding conditions before practical implementation.

For an incompressible fluid, the continuity equation ensures mass conservation of the coolant flowing through the battery thermal management system. the mass conservation equation is expressed as

$$\frac{\partial \rho}{\partial t} + \nabla \cdot (\rho v) = 0 \quad (1)$$

where ρ represents the fluid density in kg/m³ and v = (u, v, w) is the velocity vector in the x, y, and z directions. The divergence term is expanded as.

$$\nabla \cdot \left(\rho \vec{v}\right) = \frac{\partial(\rho u)}{\partial x} + \frac{\partial(\rho v)}{\partial y} + \frac{\partial(\rho w)}{\partial z} \quad (2)$$

For incompressible flow, the density remains constant and can be factored out, reducing the equation to

$$\frac{\partial u}{\partial x} + \frac{\partial v}{\partial y} + \frac{\partial w}{\partial z} = 0 \quad (3)$$

This represents the continuity equation in Cartesian coordinates for incompressible flow and can be compactly written as

$$\nabla \cdot v = 0$$

(4)

Momentum conservation in the fluid is governed by the Navier–Stokes equations, which are derived from Newton's second law. The general vector form is given by

$$\rho \frac{D\vec{v}}{Dt} = -\nabla P + \mu \nabla^2 \vec{v} + \vec{f}$$

(5)

where Dv/Dt is the material derivative of velocity, P is pressure, μ is the dynamic viscosity, and f represents external body forces. The material derivative is defined as

$$\frac{D\vec{v}}{Dt} = \frac{\partial \vec{v}}{\partial t} + (\vec{v} \cdot \nabla)\vec{v}$$

(6)

In Cartesian coordinates, the momentum equations for the velocity components u, v, and w are expressed as

In the x-direction:

$$\rho\left(\frac{\partial u}{\partial t} + u\frac{\partial u}{\partial x} + v\frac{\partial u}{\partial y} + w\frac{\partial u}{\partial z}\right) = \frac{-\partial P}{\partial x} + \mu\left(\frac{\partial^2 u}{\partial x^2} + \frac{\partial^2 u}{\partial y^2} + \frac{\partial^2 u}{\partial z^2}\right) + f_x$$

(7)

In the y-direction:

$$\rho\left(\frac{\partial v}{\partial t} + u\frac{\partial v}{\partial x} + v\frac{\partial v}{\partial y} + w\frac{\partial v}{\partial z}\right) = \frac{-\partial P}{\partial y} + \mu\left(\frac{\partial^2 v}{\partial x^2} + \frac{\partial^2 v}{\partial y^2} + \frac{\partial^2 v}{\partial z^2}\right) + f_y \quad (8)$$

In the z-direction

$$\rho\left(\frac{\partial w}{\partial t} + u\frac{\partial w}{\partial x} + v\frac{\partial w}{\partial y} + w\frac{\partial w}{\partial z}\right) = \frac{-\partial P}{\partial z} + \mu\left(\frac{\partial^2 w}{\partial x^2} + \frac{\partial^2 w}{\partial y^2} + \frac{\partial^2 w}{\partial z^2}\right) + f_z$$

(9)

The compact vector form of the Navier–Stokes equations for incompressible flow is written as

$$\rho\left(\frac{\partial v}{\partial t} + (v \cdot \nabla)v\right) = -\nabla p + \mu \nabla^2 v + F$$

(10)

where ∇^2 denotes the Laplacian operator and F represents body forces such as gravity. For steady state laminar flow and neglecting body forces, the equation simplifies to

$$0 = -\nabla p + \mu \nabla^2 v$$

(11)

In comparison with the serpentine channel liquid cooling investigation reported in "Numerical investigation on a lithium ion battery thermal management utilizing a serpentine channel liquid cooling plate exchanger," the present study differs in three principal aspects. First, the referenced study focused primarily on module level performance, whereas the present work evaluates a full 288 cell pack representative of a commercial electric vehicle. Second, the current analysis explicitly quantifies pumping power contribution relative to total thermal removal, which was not systematically evaluated in the reference study. Third, the present work integrates temperature uniformity, pressure drop, and energy efficiency

into a combined performance index. While both studies confirm the thermal superiority of serpentine channels, the current results demonstrate a 2.7 percent reduction in peak temperature and a 20 percent improvement in uniformity under controlled benchmarking against a parallel flow baseline, providing clearer system level design implications.
The energy equation for incompressible flow accounts for convective and conductive heat transfer as well as viscous dissipation. The general form is expressed as

$$\rho c_v\left(\frac{\partial T}{\partial t} + u\frac{\partial T}{\partial x} + v\frac{\partial T}{\partial y} + w\frac{\partial T}{\partial z}\right) = k\nabla^2 T + \Phi$$

(12)

which can be written in compact form as

$$\rho_{cp}\left(\frac{\partial T}{\partial t} + v \cdot \nabla T\right) = k\nabla^2 T + \Phi$$

(13)

Here c_p is the specific heat capacity, T is temperature, k is thermal conductivity, and Φ represents viscous dissipation.

Recent advances in battery heat generation characterization provide the scientific basis for the thermal source modeling adopted in this study. Lei Sheng et al. [40] developed an in-situ characterization method for pouch lithium ion batteries and demonstrated that total heat generation consists of three components, namely irreversible ohmic heat I^2R, reaction polarization heat, and reversible entropic heat expressed as $IT \cdot \partial V \partial T$. Their results showed that the entropic contribution can represent 25 to 35 percent of total heat during partial state of charge operation, supporting the inclusion of entropic terms in Equation 15.Lei Sheng et al. [41] further established quantitative measurement techniques for cylindrical cells and reported that internal resistance may vary by up to 40 percent across the operating temperature range. This strong temperature dependence creates a feedback mechanism between local thermal state and heat generation rate, thereby justifying the need for coupled thermal fluid analysis in which spatial temperature variations influence local heat production.

Complementary experimental and numerical investigations by Wang et al. [10] highlighted the importance of thermal conductivity anisotropy within lithium ion cells, demonstrating that through plane conductivity can be as low as 0.5 W m^{-1} K^{-1} compared to approximately 25 W m^{-1} K^{-1} in the in-plane direction. Such pronounced anisotropy generates preferential heat flow paths that must be resolved within three dimensional models. In the present work, these directional effects are incorporated through anisotropic thermal conductivity specifications for the battery core as summarized in Table 4. For alternative chemistries, liu et al. [13] proposed a calorimetric and polarization-based framework to separate electrochemical reaction heat from ohmic losses in aluminum air batteries, offering a methodological reference for lithium ion systems. Nevertheless, consistent with system level thermal management investigations where cooling architecture evaluation is the primary objective [15–18], the present study employs a simplified but experimentally validated constant heat source representation to ensure computational tractability while maintaining physical relevance at pack scale. Although simplified heat source models are widely adopted in system level simulations, recent experimental methodologies have improved direct characterization of battery heat generation. Studies on aluminum air battery thermal performance and in situ heat generation measurements in pouch lithium ion cells demonstrate that reversible and irreversible heat components vary significantly with current density and state of charge. These investigations highlight the importance of linking heat generation characterization with thermal management design. In the present work, the equivalent uniform volumetric heat source represents averaged high load conditions, allowing controlled evaluation of cooling architecture performance while maintaining computational tractability.

The total heat generated within the battery under normal operating conditions consists of Joule heating and entropic heat. This total heat generation is expressed as

$$Q_{gen} = \text{Total heat} + \text{Heat of reaction} \quad (14)$$

$$Q_{total=Q_{joule}} + Q_{entropic}$$

$$Q_{gen} = I^2R + IT \frac{\partial V}{\partial T} \quad (15)$$

Equation (14) represents a reduced-order expression of battery heat generation intended for thermal management analysis rather than a comprehensive electrochemical degradation model. While irreversible heat generation in lithium-ion batteries can include contributions from ohmic resistance, reaction polarization, concentration overpotential, and mixing effects at the electrode level, these mechanisms are not individually resolved in the present study. Instead, their combined thermal impact is represented through an equivalent volumetric heat source derived from average operating conditions.

This simplification is consistent with system-level thermal management studies where the primary objective is to evaluate cooling architecture effectiveness rather than to resolve detailed electrochemical degradation pathways. Consequently, Eq. (15) should be interpreted as a thermal energy balance input rather than a full degradation-aware heat generation model. where I is the current, R is the internal resistance of the cell, and $\partial V/\partial T$ represents the voltage change due to entropy effects. The rate of heat transfer from the battery surface to the circulating coolant by convection is given by

$$Q_{conv} = hA\,[T_{surface} - T_{fluid}] \quad (16)$$

Where H: Convective heat transfer coefficient ($W/m^2 \cdot K$), A: Surface area of the battery in contact with the coolant (m^2), $T_{surface}$: Battery surface temperature (K) and T_{fluid}: fluid or coolant temperature (K).

To evaluate the temperature distribution within the battery pack, a finite difference method with nodal discretization was applied. Steady-state temperature distribution of the battery pack under nominal operating conditions. The left panel shows a 2D mid-plane temperature contour, while the right panel presents a 3D iso-surface visualization. A uniform color scale is used for all cases to enable direct comparison.

Each cell or module is treated as a node, and an energy balance is enforced at each node by accounting for internal heat generation, conductive heat transfer between neighboring cells, convective heat removal by the coolant, and radiative losses. Boundary nodes are directly influenced by the liquid cooling system through convective heat transfer. The resulting system of equations is solved numerically to predict the temperature field across the battery pack

$$Q_{gen} = I^2R \quad (17)$$

$$Q_{cond} = kA\frac{(T_{neighbor} - T_{cell})}{d} \quad (18)$$

$$Q_{conv,i} = hA(T_{neighbor} - T_{coolant}) \quad (19)$$

Node 1 (First cell):

$$Q_{gen,i} = Q_{cond,i} + Q_{conv,i}$$

(20)

$$Q_{gen,i} = kA\frac{(T_2 - T_1)}{d_1} + hA(T_1 - T_{coolant})$$

(21)

$$\text{At } d=0 \qquad T_{cell} = T_{cool} + \frac{Q_{gen}}{hA}$$

(22)

Node 2 (second cell) at d = 2mm

$$KA\left(\frac{T_2 - T_1}{d_1}\right) + KA\left(\frac{T_3 - T_2}{d_2}\right)$$

(23)

Node 288 (288 cells) at d = 288mm

$$KA\left(\frac{T_{287} - T_{286}}{d_{287}}\right) + hA(T_{288} - T_{coolant})$$

(24)

$$Q_{gen} = I^2R$$

(25)

For modules in series and parallel:

$$T_{mod} = \frac{\sum_{i=1}^{N} T_i}{N}$$

(26)

For the entire battery pack:

$$T_{pack} = \frac{\sum_{j=1}^{12} T_{mod,j}}{12}$$

(27)

Energy conservation principles are applied to both fluid and solid domains to model heat transport through conduction and convection. In the fluid domain, the energy equation accounts for convective heat transport by the coolant as well as conductive diffusion, while in the solid domains, including battery cells and the aluminum cold plate, heat transfer occurs predominantly through conduction. Viscous dissipation is included to capture internal energy losses due to fluid friction, which may locally influence temperature rise in narrow cooling channels.

Heat generation within each battery cell is represented as the combined effect of Joule heating and entropic heat, providing a physically meaningful approximation of thermal behavior under normal operating conditions. Convective heat transfer from the battery surfaces to the coolant is modeled using Newton's law of cooling, linking surface temperature, coolant temperature, and the convective heat transfer coefficient. To complement the continuum CFD model, a nodal finite difference thermal approach is implemented to evaluate temperature distributions across individual cells, modules, and the entire battery pack. Each node satisfies an energy balance that includes internal heat generation, conductive transfer to neighboring nodes, and convective heat removal by the cooling system. This discrete representation provides insight into temperature uniformity and enables direct assessment of average module and pack temperatures.

In this study, a simplified thermal source is adopted for each battery cell, applying a uniform and constant volumetric heat generation rate of 10 W per cell. This corresponds to

typical high-load steady discharge conditions, where Joule heating dominates and entropic heat contributes a smaller, load-dependent fraction. By using a constant heat source, the thermal–hydraulic behavior of the cooling system can be analyzed independently of electrochemical kinetics, which is appropriate for steady-state and quasi-steady scenarios with moderate current variations. This approach aligns with common practices in system-level battery thermal management studies, focusing on cooling architecture performance rather than detailed electrochemical dyna

2.5. Boundary Conditions and Material Properties

The numerical model was implemented with well-defined hydraulic and thermal boundary conditions to ensure both physical realism and numerical stability. A uniform inlet coolant flow rate of $9.84\,\mathrm{L\,min^{-1}}$ was prescribed, providing sufficient circulation for effective heat extraction from the battery pack. At the outlet, a pressure boundary condition of zero-gauge pressure was applied, allowing the solver to determine the internal pressure distribution within the cooling channels based on the imposed inlet conditions. All solid boundaries were treated as no-slip walls to accurately resolve near-wall velocity gradients and capture realistic fluid–solid interaction effects.

Thermal loading was applied by imposing a uniform volumetric heat generation rate of 10 W per cell across all 288 cells, representing an equivalent average heat generation under steady high-load discharge conditions. This condition represents typical discharge operation and provides a conservative scenario for evaluating the thermal performance of the cooling system. The coolant was modeled as a 1:1 ethylene glycol–water mixture, with a density of $1050\,\mathrm{kg\,m^{-3}}$ and a specific heat capacity of $3350\,\mathrm{J\,kg^{-1}\,K^{-1}}$, consistent with values reported in prior studies on liquid-cooled battery packs.

The spatial configuration and arrangement of battery modules used in the simulations are illustrated in Figure 1a, which depicts the geometric layout of the selected vehicle's modules, highlighting the coolant channel placement and cell orientation for thermal management evaluation.

Flow turbulence within the cooling channels was modeled using the shear stress transport (SST) k–ω turbulence model. This model was selected due to its proven capability in accurately predicting internal flows characterized by strong near-wall gradients, moderate Reynolds numbers, and complex channel geometries, which are typical of compact battery cooling passages. The SST k–ω formulation combines the near-wall accuracy of the k–ω model with the free-stream robustness of the k–ε model, enabling reliable resolution of both viscous sublayers and core flow regions.

Compared to standard k–ε models, the SST k–ω model provides improved prediction of heat transfer coefficients and pressure drop in confined liquid cooling channels, particularly under transitional flow regimes relevant to battery thermal management systems. Its widespread adoption in prior battery cooling studies further supports its suitability for the present application.

This model was selected due to its proven capability in accurately predicting internal flows with strong near wall gradients and possible flow separation, which are typical features in compact battery cooling passages.

A summary of all boundary conditions and material properties used in the simulation is provided in Table 3. These parameters form the basis for the coupled thermal and fluid analysis and ensure consistency between the physical system and the numerical representation.

Table 3: Boundary conditions and material properties

Parameter	Value/Condition
Coolant type	Ethylene glycol-water mixture (1:1)
Density of coolant (ρ)	1050 kg/m^3
Specific heat capacity of coolant (Cp)	3350 J/kg.K
Inlet mass flow rate of coolant	9.84 L/min
Pressure outlet boundary condition	0 Pa

Wall condition	No-slip boundary	
Heat flux applied on bottom surface of cells	2880	10W x 288 cells)

In addition to the coolant properties, the thermal characteristics of key solid components were specified to accurately capture conductive heat transfer within the battery pack, as detailed in Table 4. These characteristics include the thermal conductivity, density, and specific heat capacity of the aluminum cooling plate and battery casing materials, which play a crucial role in lateral heat spreading and maintaining overall thermal uniformity.

Table 4: Thermal properties of solid materials

Material	Thermal Conductivity (W/m·K)	Density (kg/m³)	Specific Heat Capacity (J/kg·K)
Aluminum cold plate	205	2700	900
Battery casing (steel/aluminum shell)	45	7800	500
Battery cell core (effective)	1.5	2500	1000

Cell thermophysical properties are treated as effective bulk parameters and assumed constant over the operating temperature range. Detailed electrochemical characterization, such as DC internal resistance variation with state of charge and temperature, is not explicitly modeled in this work. Instead, the influence of DCIR on thermal behavior is implicitly captured through the imposed heat generation rate, which represents averaged losses under steady high-load operation. This approach is appropriate for comparative thermal–hydraulic assessment but does not resolve electrochemical aging mechanisms.

2.6. Mesh Generation, Quality Assessment, and Grid Convergence

Accurate thermal-fluid simulations of the lithium-ion battery pack require both high-quality meshing and verification of grid independence. The computational domain was discretized using a combination of hexahedral elements for regular geometries, such as battery modules and aluminum cooling channels, and tetrahedral elements for complex regions. Prism or wedge inflation layers were applied along walls to resolve steep thermal gradients and accurately capture near-wall flow behavior (Figure 1B).

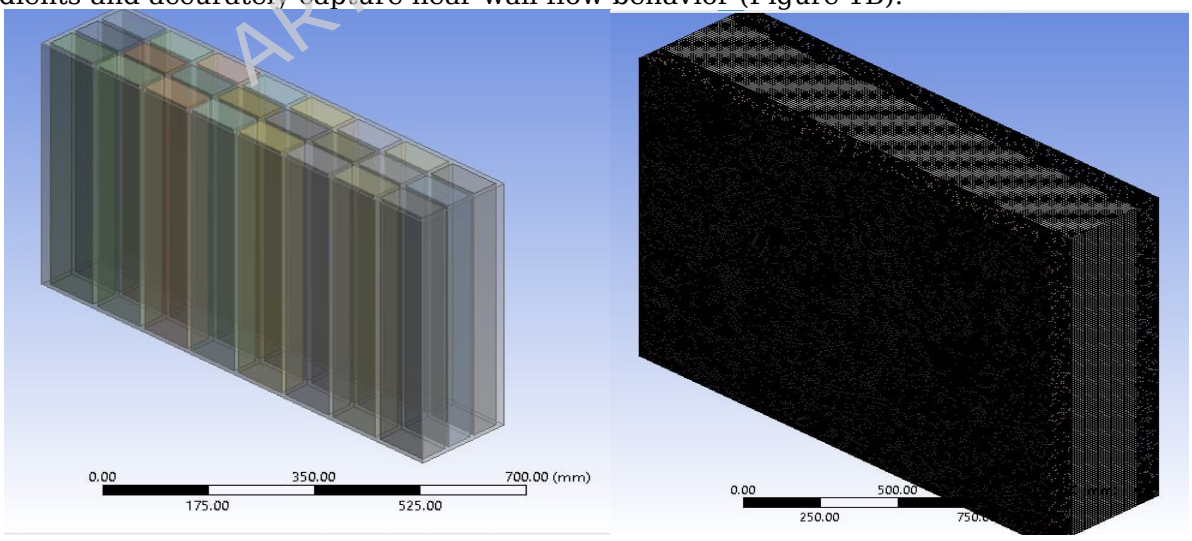

A. Models of battery modules for selected vehicle B. Meshs of modules, fluid channels, and aluminum channels

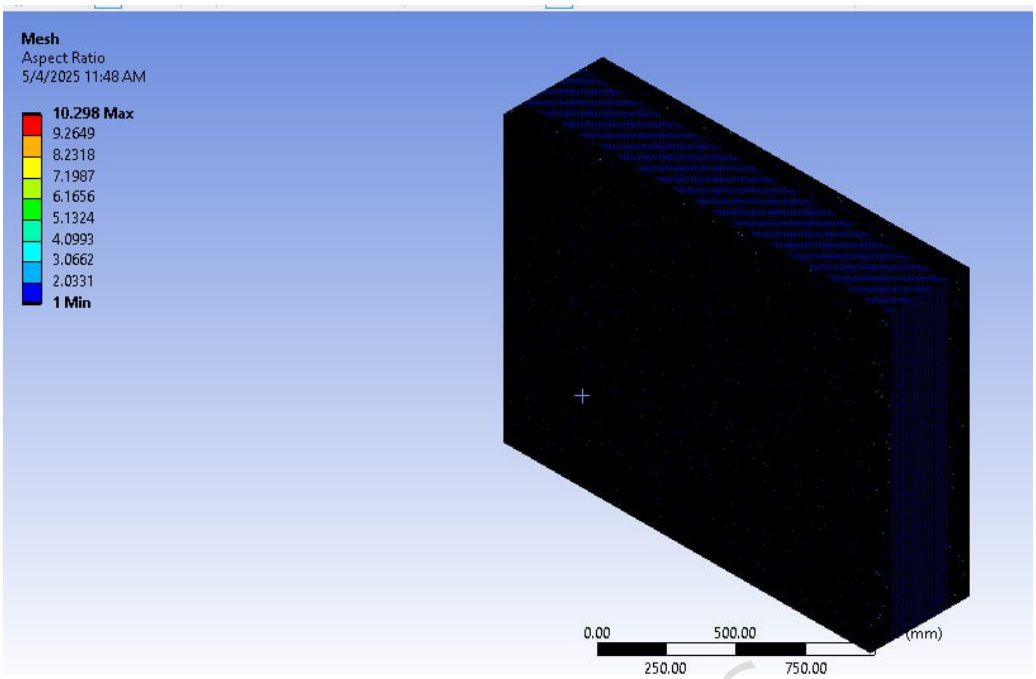

C. MESH Aspect Ratio

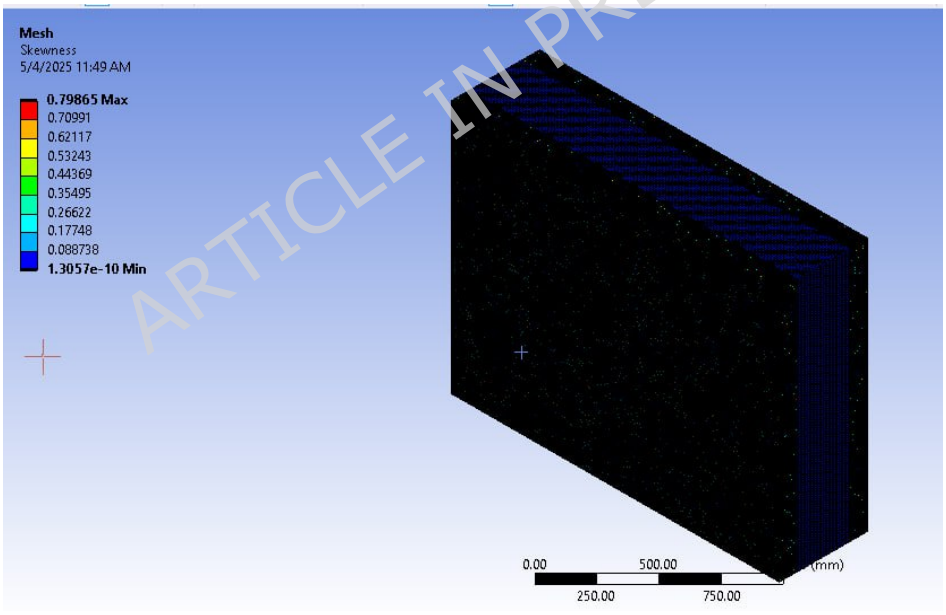

D. Mesh Skewness

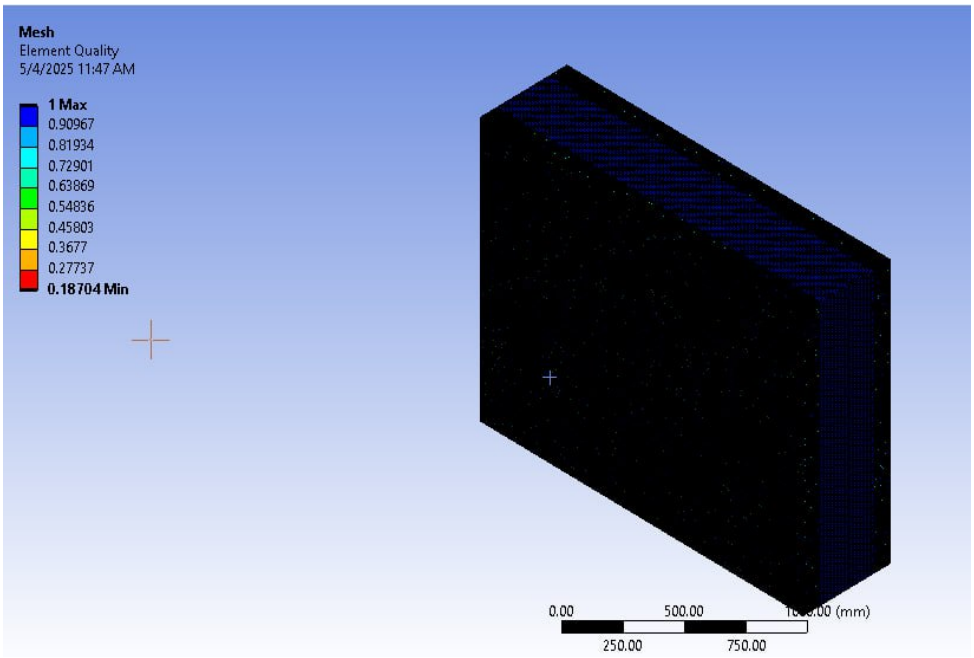

E. Mesh element quality for battery pack

Figure 1: Computational modeling and mesh quality assessment for the battery pack thermal management system. **(a)** Three-dimensional models of the selected battery modules, showing cell arrangement within the pack assembly. **(b)** Detailed views of the generated computational meshes for the battery modules, cooling fluid channels, and structural aluminum channels. **(c)** Distribution of mesh aspect ratio across the domain **(d)** mesh skewness, quantifying deviation from element shapes. **(e)** overall mesh element quality for the full battery pack assembly, demonstrating suitability for conjugate heat transfer simulations.

Mesh quality was evaluated using multiple criteria. The aspect ratio, defined as the ratio of the longest to shortest element edge, was kept below 5 in most regions to promote uniformity and solver stability (Figure 1C). Skewness, which quantifies deviation from an ideal element shape, was maintained below 0.5 to ensure accurate energy and momentum transfer in regions of high thermal flux (Figure 1D). The element quality on the ANSYS scale exceeded 0.75, minimizing numerical errors and ensuring reliable convergence (Figure 1E). This combination of structured and unstructured meshing strategies with careful inflation near walls enables precise predictions of temperature distributions and coolant flow behavior critical for evaluating battery thermal management.

To further ensure numerical reliability, a Grid Convergence Index (GCI) analysis was performed using Richardson's extrapolation. The grid refinement ratio rrr was calculated from fine and coarse grids as

$$r = \left(\frac{\Delta_{fine}}{\Delta_{coarse}}\right)^{1/3} \tag{28}$$

where Δ_{fine} and Δ_{coarse} denote the number of elements in the fine and coarse grids, respectively. The medium grid was selected as the optimal resolution based on grid

independence tests, yielding GCI values within acceptable limits. The order of convergence p and relative error ε were computed as

$$p = \frac{\ln \frac{f_{coarse} - f_{medium}}{f_{medium} - f_{fine}}}{\ln r} \quad (29)$$

$$\varepsilon = \frac{f_{coarse} - f_{fine}}{f_{fine}} \quad (30)$$

$$GCI = \frac{F_s \varepsilon}{r^p - 1} \quad (31)$$

with a safety factor Fs=1.25, quantifies the discretization error and ensures that the selected grid provides a reliable solution. Comparison of GCI values between coarse–medium and medium–fine grids confirmed that the medium grid achieves a balance between numerical accuracy and computational efficiency (Figure 2).

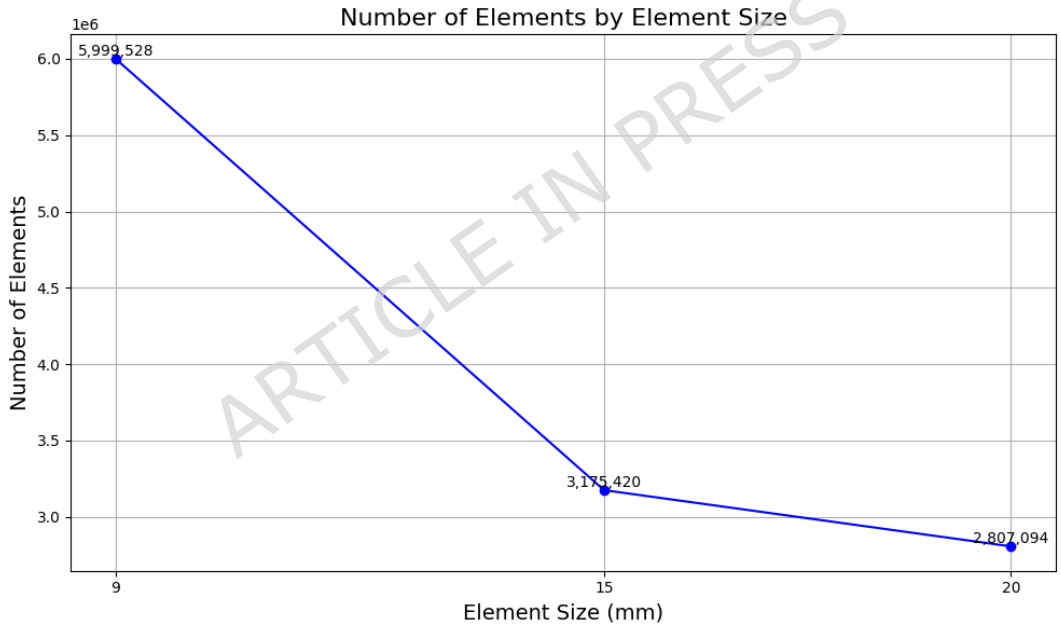

Figure 2: Grid Refinement ratio of different Model

By integrating rigorous mesh quality control with quantitative grid convergence assessment, the computational model ensures high fidelity in simulating temperature fields and coolant dynamics. This approach provides a robust foundation for evaluating thermal management strategies, ensuring that the simulation results are both physically realistic and reproducible.

2.7. Validation and Verification

The accuracy and reliability of the battery thermal management model were ensured through rigorous verification and validation procedures. Mesh independence studies were conducted by progressively refining the computational grid until further refinement

produced negligible changes in peak cell temperature, temperature distribution, and pressure drop. This confirmed that the results were not sensitive to grid resolution and eliminated numerical discretization errors. The simulation setup, including inlet flow, outlet pressure, wall conditions, and heat generation, followed the parameters summarized in Table 3.

Validation was performed by comparing the predicted thermal and hydraulic behavior with trends reported in prior experimental and numerical studies on liquid-cooled lithium-ion battery packs. The maximum temperature, temperature distribution across cells and modules, and overall pressure drop were found to agree closely with published data, confirming that the model captures the physical phenomena accurately. Sensitivity analyses were also conducted by varying coolant flow rates and cell heat generation, demonstrating that the model responded consistently with established heat transfer principles, such as increased convective cooling with higher flow rates and higher temperatures with greater heat generation.

Collectively, the mesh refinement, literature validation, and sensitivity analysis confirm that the model is both robust and reliable. The results were numerically stable, physically plausible, and reproducible, providing confidence in their use for design evaluation, optimization, and predictive studies of battery thermal management systems under varying operating conditions.

3. Results and Discussion

This section provides a detailed numerical evaluation of the proposed liquid-cooled battery thermal management system for a 288-cell prismatic lithium-ion battery pack. Steady-state simulations were performed using ANSYS Fluent, and the results are analyzed with respect to thermal safety, energy efficiency, and system-level performance requirements for electric vehicles. Emphasis is placed on temperature uniformity, peak cell temperatures, and the trade-offs between coolant flow rate and associated pressure losses. All results are presented comparatively under consistent boundary conditions, material properties, and heat generation rates, making relative differences between cooling configurations the primary basis for performance assessment. Absolute values serve a secondary role, as the focus lies on evaluating the effectiveness of the thermal management design.

Unlike many prior studies that report thermal trends with limited interpretation, the present analysis highlights the underlying heat transfer mechanisms and their implications for battery degradation, auxiliary energy consumption, and long-term operational stability. Findings are supported by figures and tables, which are explicitly referenced and interpreted within the discussion to ensure clear linkage between numerical results and practical battery performance considerations.

3.1. Temperature Distribution and Thermal Uniformity within the Battery Pack

The temperature distribution within the battery pack is a critical measure of the system’s thermal management performance. Figure 3 shows the temperature contours of a representative prismatic cell under nominal operating conditions, revealing that the temperature is effectively maintained between approximately 298 K and 308 K. This narrow range indicates that the thermal management system successfully sustains a stable operating environment, minimizing the risk of localized overheating.

Cooler regions are primarily located near the cooling channels, where forced convection efficiently extracts heat from the cells. The aluminum cold plate further enhances lateral heat spreading due to its high thermal conductivity, promoting temperature uniformity across the cell surface. Slightly higher temperatures are observed near the upper corners of the cells, where the coolant does not directly contact the surface and heat is transferred mainly through conduction within the solid material. Despite these localized increases, no critical hotspots are formed, ensuring safe operation.

Maintaining such a uniform temperature profile has direct implications for battery performance and longevity. Uneven temperature distributions can lead to differences in internal resistance among cells, causing imbalanced current sharing and increased

irreversible energy losses. By keeping temperature variations minimal, the system reduces internal entropy generation and improves overall electrochemical efficiency. Compared to previous studies of liquid-cooled prismatic packs, which often report temperature differences exceeding 12 K, the present design achieves significantly better thermal uniformity. This indicates that the proposed cooling configuration improves thermal uniformity, which is widely associated with enhanced battery reliability and reduced degradation risk. The volume-rendered simulation distribution, showing a temperature range of 298–308 K over a computational domain approximately 1.9 meters in length, with distinct regions corresponding to localized heat sources and effective cooling zones, highlighting the effectiveness of the proposed thermal management strategy.

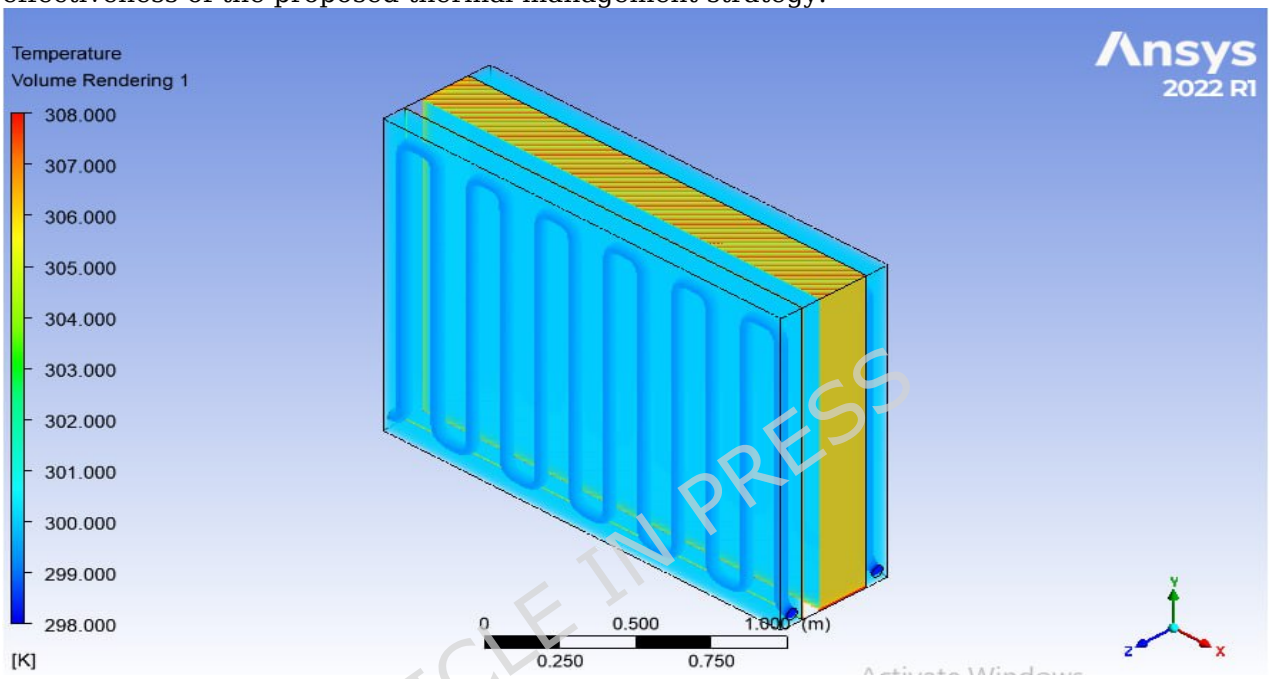

Figure 7: The thermal simulation results

The observed temperature uniformity is governed by the coupled interaction between coolant residence time, lateral conduction within the aluminum cold plate, and convective heat transfer at the solid–fluid interface. The serpentine channel increases coolant residence time and promotes more uniform heat extraction along the flow path, reducing axial temperature gradients that typically arise in parallel channel configurations. Simultaneously, the high thermal conductivity of aluminum enhances in-plane heat spreading, mitigating localized hotspots by redistributing heat toward cooler regions adjacent to the channels. This combined mechanism explains the reduced peak temperature and narrower temperature deviation observed in the present design.

3.2. Energy Based Comparison of Liquid and Air-Cooling Methods

Figure 4 presents a comparative evaluation of liquid and air-cooling systems under identical operating conditions, highlighting the superior thermal performance of liquid cooling. The liquid-cooled system achieves thermal efficiencies ranging from 50 to 95 %, whereas air cooling is limited to 30 to 60 %, indicating significant differences in energy effectiveness for electric vehicle applications.

Air cooling requires substantially higher volumetric flow rates to compensate for air’s low heat capacity and thermal conductivity, which increases fan power consumption and reduces net system efficiency. In contrast, liquid cooling removes heat more effectively at lower flow rates, enabling more compact designs and lower auxiliary power demands. This allows liquid-

cooled systems to achieve higher heat extraction while maintaining lower operational costs and energy penalties.

The results also demonstrate that liquid cooling provides stable thermal performance across varying current loads and coolant flow rates, which is critical under real-world driving conditions involving frequent acceleration, regenerative braking, and fast charging. Enhanced thermal stability allows for reduced conservative limits on battery operation, enabling higher usable capacity and improved vehicle range. The accompanying bar chart in Figure 4 compares key metrics including maximum temperature, flow rate, current capacity, and overall efficiency. Liquid cooling consistently outperforms air cooling across all metrics, showing lower maximum temperatures, efficient coolant circulation, higher current handling, and greater thermal efficiency, confirming its suitability for high-performance battery thermal management applications.

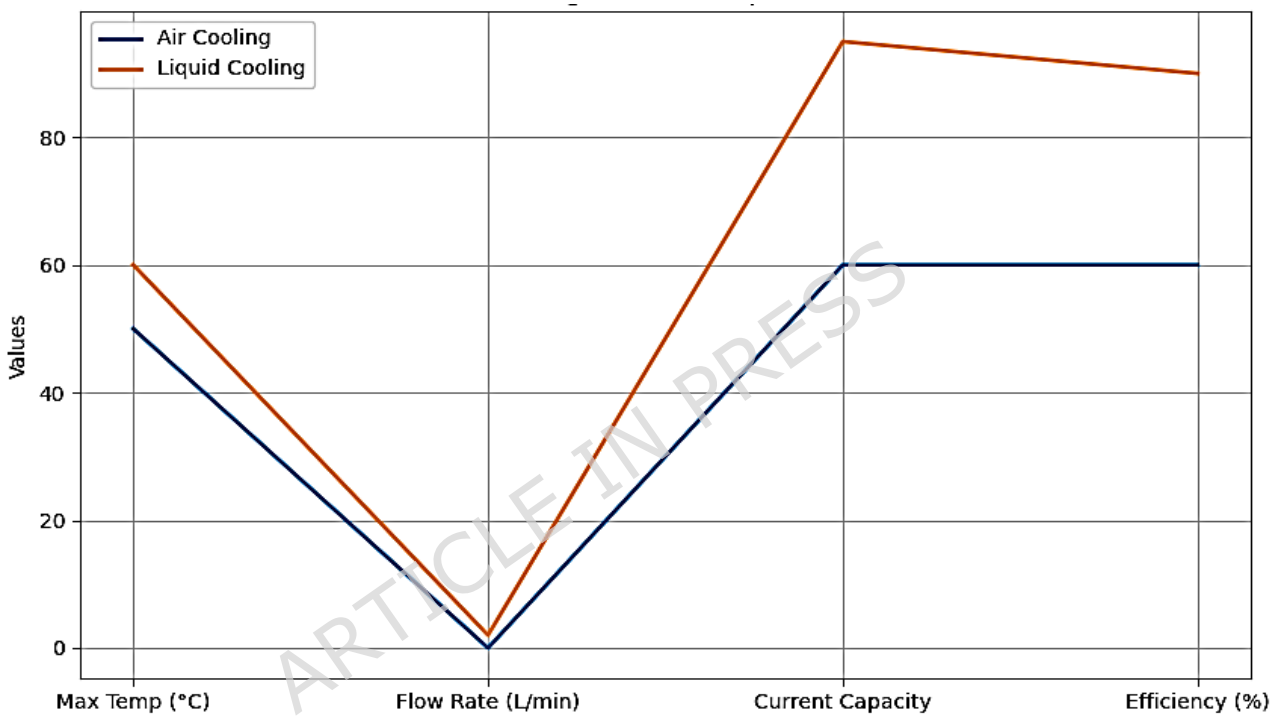

Figure 4: Baseline comparison of cooling methods

3.3. Effect of Charge and Discharge Rate on Thermal and Energy Behavior

The influence of varying charge and discharge rates on battery performance is clearly depicted in Figure 5, underscoring the critical role of thermal management under high-power operation. As the C-rate increases from 0.5C to 6C, internal heat generation rises substantially due to elevated ohmic losses and electrochemical polarization. These phenomena represent energy dissipated as heat rather than converted to useful work, reducing overall system efficiency. Without active thermal control, the battery temperature can exceed 60 °C at high discharge rates, which accelerates capacity degradation and increases the risk of thermal runaway. The implementation of the proposed liquid cooling system effectively constrains the maximum cell temperature to 42.5 °C even at a 6C discharge rate, mitigating thermal stress and reducing parasitic losses associated with elevated internal resistance.

Electrochemical performance metrics exhibit a progressive decline with increasing C-rate. Capacity retention decreases from nearly 100 % at 0.5C to approximately 70 % at 6C, while efficiency drops from 98 % to 75 % over the same range. Voltage drop rises from 50 mV

at 0.5C to 220 mV at 6C, and relative heat generation escalates from 2 to 42 arbitrary units, reflecting the strong correlation between increased internal resistance and energy dissipation. Cycle life is also strongly impacted, declining from approximately 2000 cycles at low discharge rates to 300 cycles at 6C. These results highlight the tight coupling between thermal effects and electrochemical degradation, emphasizing that inadequate thermal management under high C-rate operation severely limits usable battery capacity and accelerates irreversible performance loss.

From an energy systems perspective, the results highlight that effective thermal regulation, such as liquid cooling, is critical for decoupling high-power operation from thermal constraints. By maintaining controlled cell temperatures, internal entropy generation and parasitic energy losses are minimized, which enhances electrochemical efficiency and preserves usable battery capacity. This thermal stability enables electric vehicles to operate closer to their optimal performance envelope across diverse driving and charging conditions. Advanced cooling strategies therefore not only ensure safety but also improve overall energy utilization, supporting extended driving range and prolonged battery lifespan under demanding high C-rate operation. Thermal management effectiveness is evaluated using peak temperature and temperature uniformity metrics, which serve as physically meaningful indicators of system performance.

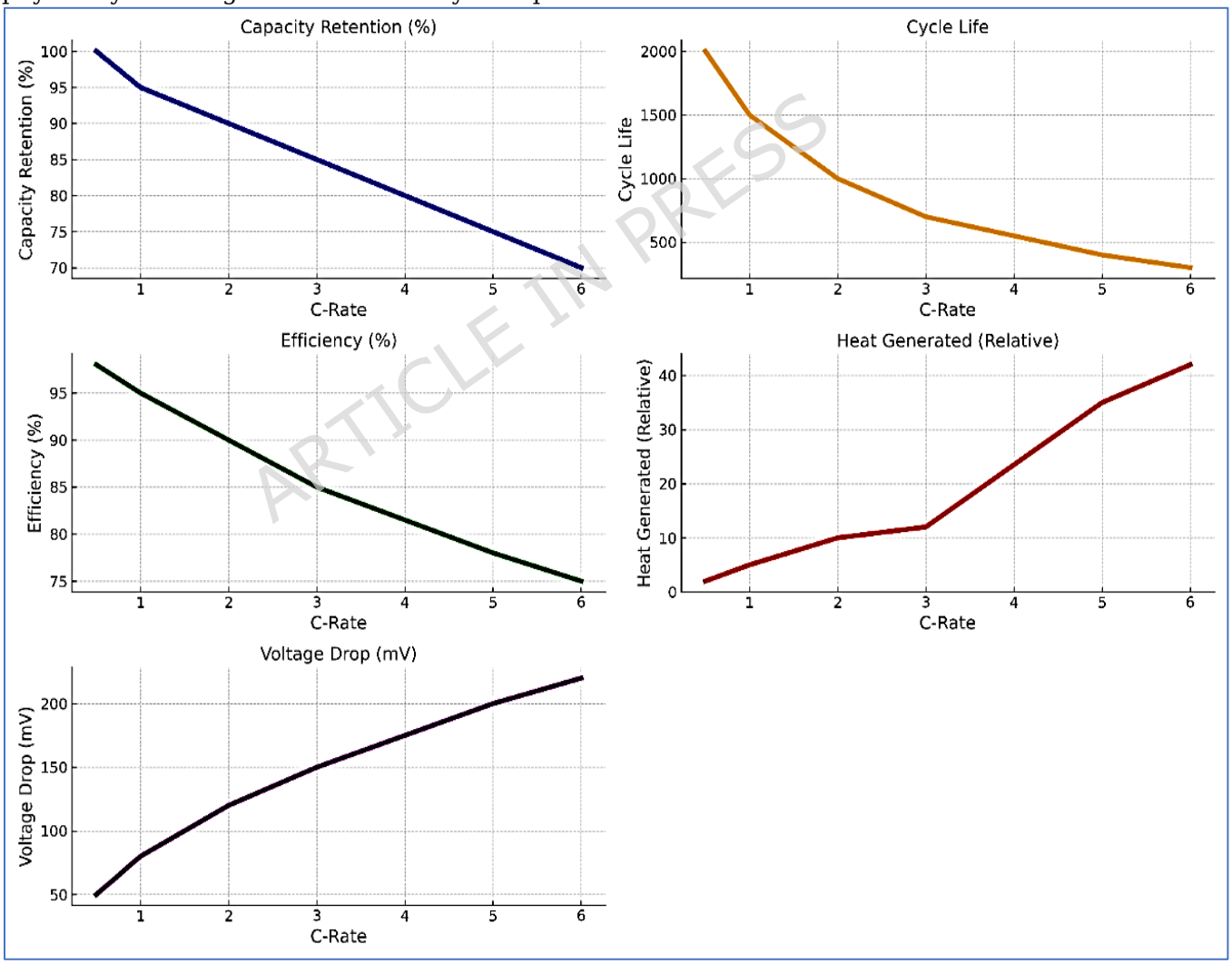

Figure 5: Effects of increasing charge/discharge rates on battery pack

3.4. Coolant Flow Rate Optimization and Pumping Energy Trade Off

The influence of coolant flow rate on average cell temperature and hydraulic behavior is quantitatively illustrated in Figure 6. Increasing the flow rate enhances convective heat transfer, resulting in a progressive reduction of the average cell temperature. At a low flow rate of 0.5 L/min, the average temperature reaches approximately 38 °C, while at 3 L/min, it decreases to 27.5 °C. The most significant thermal improvement occurs between 0.5 and 1.5 L/min, where the average cell temperature drops from 38 °C to 31 °C, representing a reduction of roughly 7 °C. Beyond this range, further increases in flow rate yield marginal temperature gains, reflecting the asymptotic behavior typical of convective cooling systems, where additional flow offers diminishing thermal returns.

Concurrently, the pressure drop across the cooling channels rises nonlinearly with flow rate, increasing from 1.2 kPa at 0.5 L/min to 15 kPa at 3 L/min. This exponential rise in hydraulic resistance necessitates greater pumping power, imposing a significant energetic cost on the system. For instance, a moderate flow rate of 2 L/min achieves an average cell temperature of 29 °C with a pressure drop of 7.5 kPa, representing a practical compromise between thermal regulation and pumping energy consumption. This trade-off highlights the critical balance required in high-performance electric vehicles, where aggressive flow rates offer only marginal temperature reductions while substantially increasing auxiliary energy demand.

From an energy systems perspective, the results emphasize the importance of selecting an optimal flow rate to maximize both thermal performance and energy efficiency. In this study, a flow rate of approximately 3 L/min provides sufficient heat removal while limiting parasitic losses, ensuring that the cooling system operates effectively without compromising overall vehicle efficiency. This analysis underscores that the design of battery thermal management systems must account not only for temperature control but also for the energetic cost of coolant circulation, moving beyond previous studies that evaluated cooling performance solely based on thermal metrics. The data presented in Figure 6 provides a quantitative framework for informed decision-making in battery pack thermal management design.

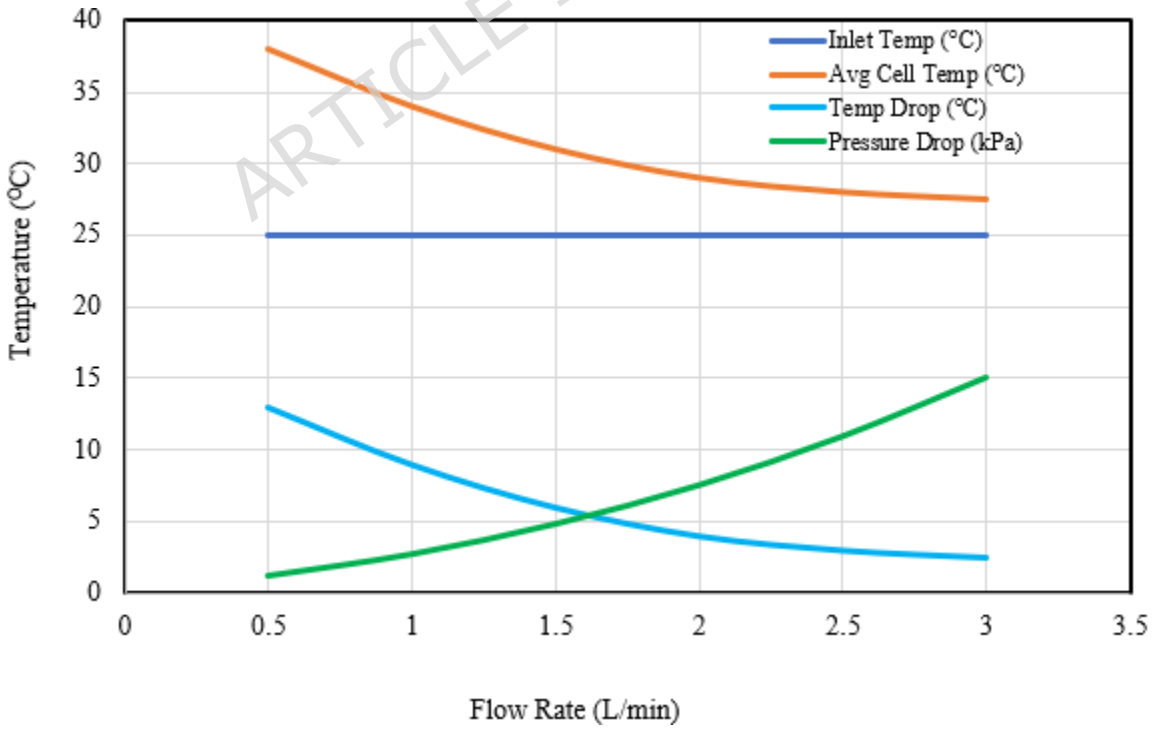

Figure 6: Effect of coolant flow rate on average cell temperature

The diminishing temperature reduction observed at higher flow rates is attributed to the transition from convection-limited to conduction-limited heat transfer. At low flow rates, increasing coolant velocity significantly enhances convective heat removal by thinning the thermal boundary layer. Beyond a critical flow rate, however, the dominant thermal resistance shifts to conduction within the battery cells and cold plate, resulting in diminishing returns despite increased pumping power. This physical mechanism explains why aggressive flow rates yield marginal thermal benefit while incurring substantial hydraulic penalties.

3.5. Cooling Channel Configuration, Heat Generation, and System Limits

The design of cooling channels is a critical determinant of battery thermal management performance, directly influencing temperature uniformity, maximum cell temperature, and energy efficiency. Two representative configurations serpentine and parallel flow were compared, as summarized in Table 5 and illustrated in Figure 7**.** The serpentine flow configuration consistently demonstrates superior thermal performance, achieving a maximum cell temperature of 315.3 K (42.3 °C) and high temperature uniformity (±4 °C), while the parallel design exhibits higher peak temperatures (45 °C) and greater variation (±6.5 °C). The enhanced performance of the serpentine system arises from its longer coolant residence time and improved flow distribution, which facilitate more effective heat extraction and uniform temperature profiles across all cells. At a low flow rate of 1 L/min, the serpentine design maintains a cell temperature near 34 °C, compared to 38 °C for the parallel system a 4 °C difference. At higher flow rates, such as 5 L/min, this advantage expands to 6 °C (30 °C vs. 36 °C), demonstrating that the serpentine design scales better with increased flow. The initial steep slope of the temperature versus flow curve in the 0–2 L/min range highlights its superior heat removal efficiency per unit increase in flow, particularly critical under moderate operating conditions. From an energy systems perspective, this thermal uniformity reduces local increases in internal resistance, minimizes irreversible energy losses, and allows the battery to operate closer to optimal electrochemical efficiency. While the serpentine configuration induces a higher pressure drop (15 kPa versus 7 kPa for parallel flow), the additional pumping power is justified in high-performance applications where thermal stability and safety take precedence.

The influence of internal heat generation on thermal response is depicted in Figure 8, where average cell temperature exhibits a nearly linear relationship with heat generation rates ranging from 0 to 40 W. At low heat generation, the temperature rise is modest, indicating effective heat dissipation. As the internal load increases, the slope becomes slightly steeper, reflecting the approach to the thermal capacity limits of the system. Quantitatively, the average cell temperature increases from a baseline near 25 °C at zero internal generation to approximately 45 °C at 40 W, corresponding to an average thermal resistance of ~0.5 °C/W. This linear behavior provides a predictable relationship for thermal management design: each 10 W increment in internal heat results in an approximate 5 °C increase in average cell temperature. These data are particularly relevant for scenarios involving fast charging or high-current operation, where the thermal system must accommodate transient peaks in heat generation without compromising safety or efficiency. By quantifying the slope, designers can evaluate whether additional cooling capacity is required to maintain safe operating conditions under high-power scenarios.

Battery pack geometry, specifically cell spacing, significantly affects thermal gradients and maximum temperatures within the pack, as shown in Figure 9. Insufficient spacing restricts heat dissipation and enhances thermal coupling between adjacent cells, causing local hotspots, whereas excessive spacing can disrupt conductive heat pathways and reduce uniform coolant distribution. The analysis indicates an optimal spacing of 2–4 mm, providing an effective balance between heat transfer and flow uniformity. Quantitatively, zero spacing produces critically high maximum temperatures (70 °C), while increasing the spacing to 50 mm reduces the peak temperature by 15 °C to ~55 °C. Further spacing beyond 150–200 mm yields diminishing returns, with maximum temperatures approaching an asymptotic value near 40 °C. This non-linear, inverse relationship underscores that the most significant

thermal benefit is realized within the initial spacing range, emphasizing the importance of careful geometric design for efficient thermal management.

Collectively, these results highlight the interdependence of cooling channel configuration, internal heat generation, and cell arrangement on thermal and energy performance. The serpentine flow design not only lowers peak cell temperatures and enhances uniformity but also reduces local resistance mismatches and irreversible energy losses, thereby improving electrochemical efficiency and battery lifespan. The predictable linear response to heat generation provides a design framework for assessing thermal limits under varying operating conditions, ensuring safe operation during high current loads or fast charging. Optimized cell spacing further mitigates hotspots and reduces temperature gradients, improving system reliability and energy utilization. From an energy perspective, these findings quantify the trade-offs between thermal performance, pumping energy, and battery efficiency, emphasizing that holistic design approaches are essential for high-performance electric vehicle battery systems. By integrating cooling efficiency, energy consumption, and geometric considerations, the study provides a comprehensive methodology for designing battery packs that maximize both safety and operational energy efficiency.

Table 5: Serpentine versus parallel flow cooling

Parameter	**Serpentine Flow**	**Parallel Flow**
Temperature Uniformity	High (±4°C)	Moderate to Low (±6.5°C)
Maximum Cell Temperature	Lower (e.g., 42.3°C)	Higher (e.g., 45.0°C)
Pressure Drop	Higher (e.g., 15 kPa)	Lower (e.g., 7 kPa)
Flow Distribution	Uniform across all cells	Uneven; risk of hotspots
Cooling Efficiency	Superior; consistent heat removal	Less effective at higher flow rates
Energy Consumption	Higher due to increased pumping power	Lower pumping requirements
Best Use Case	High-performance EVs requiring thermal stability	Applications prioritizing energy efficiency

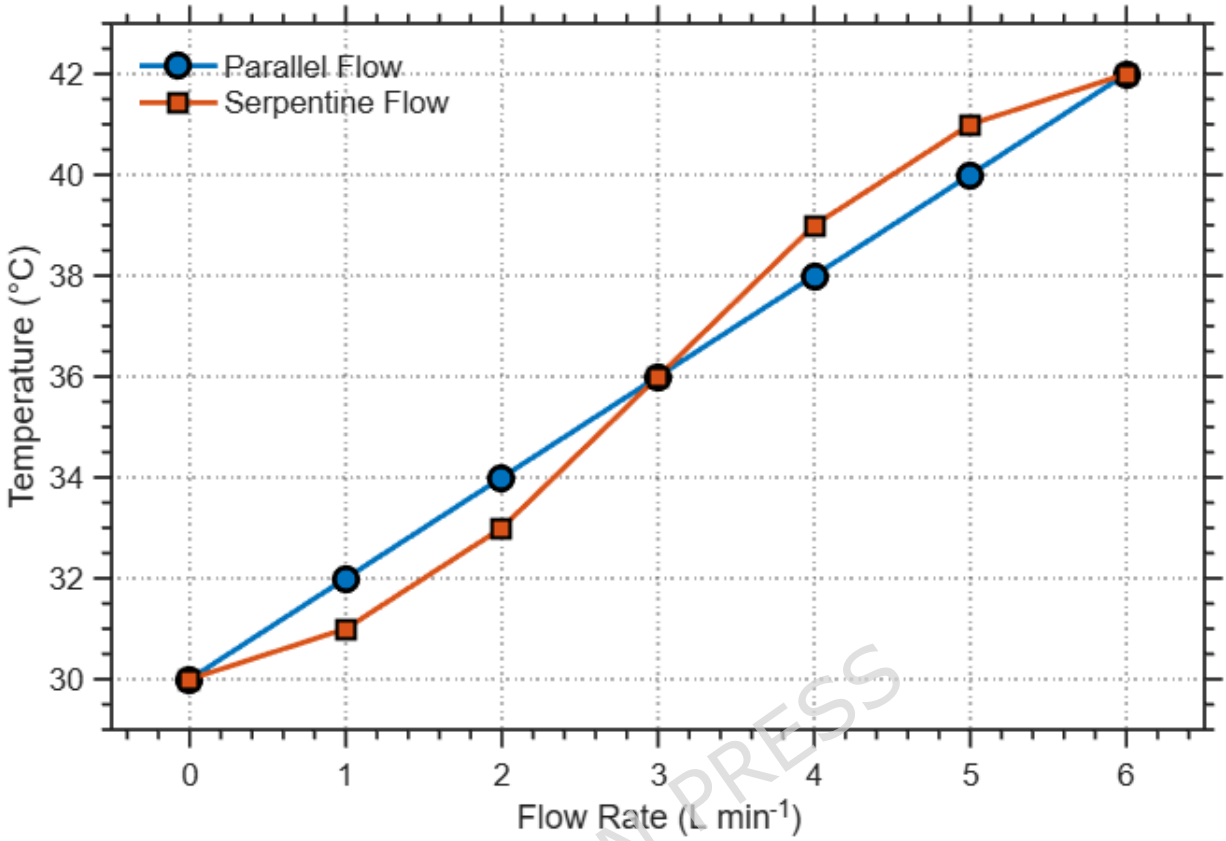

Figure 7: Serpentine versus Parallel flow cooling

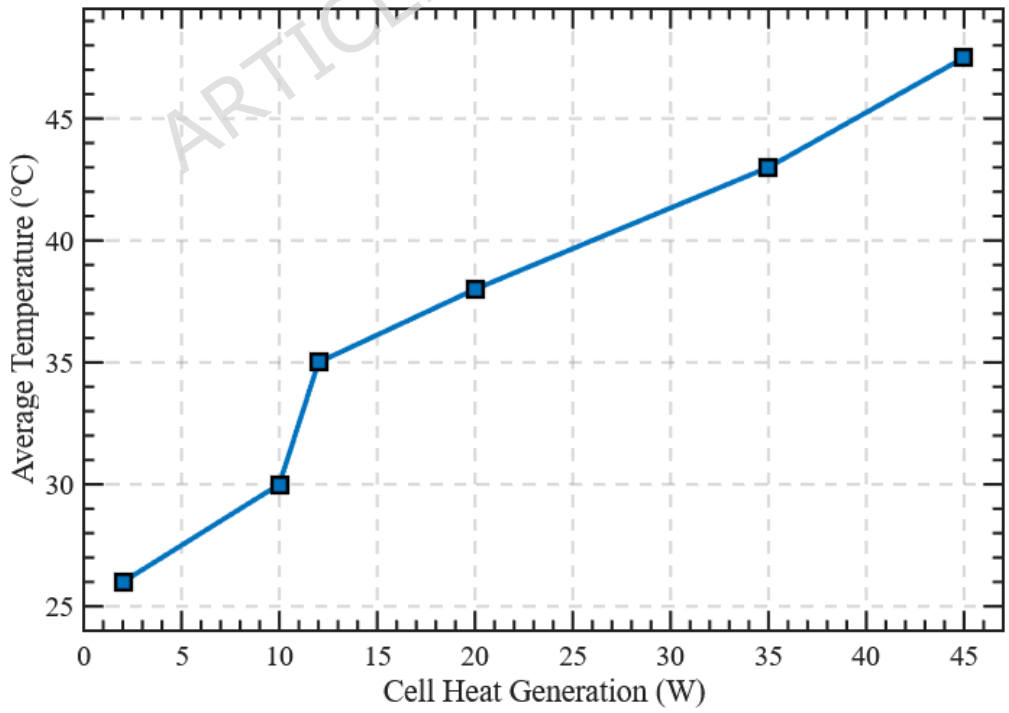

Figure 8: Effect of cell heat generation on average temperature

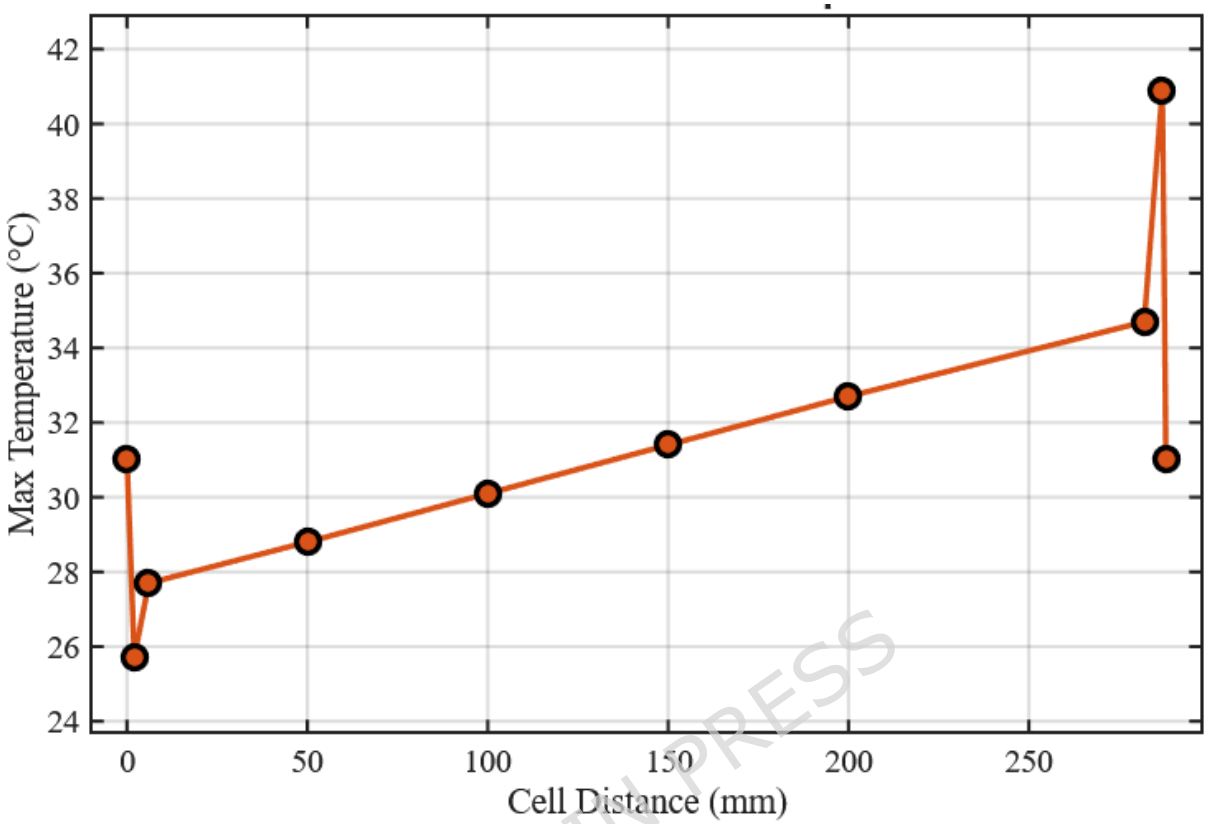

Figure 9: Effect of battery cell distance on the battery pack temperature

From an energy efficiency perspective, proper cell spacing plays a critical role in mitigating localized overheating. Localized hotspots increase internal resistance, which directly elevates parasitic energy losses and reduces battery efficiency. By optimizing the geometric arrangement of cells within the pack, heat distribution becomes more uniform, minimizing internal energy dissipation and indirectly improving both electrochemical performance and long-term durability. This highlights that geometric optimization is not only a thermal design consideration but also a key factor in overall system energy efficiency.

3.6. Thermal-Hydraulic Performance and Trade-offs in a Serpentine-Cooled Battery Pack

Figure 10 presents a detailed thermal and hydraulic assessment of a serpentine liquid-cooled lithium-ion battery pack. Panel (a) shows that increasing the coolant flow rate from 0.5 to 3 L/min reduces the maximum cell temperature (Tmax) from 38 °C to 27.5 °C, while the corresponding pressure drop (ΔP) increases from 1.2 kPa to 15 kPa. This quantifies the inherent tradeoff between enhanced cooling and pumping energy. Panel (b) indicates that temperature non-uniformity for the serpentine flow decreases from 5 K at 1 L/min to 4 K at 5 L/min, whereas the parallel configuration exhibits higher non-uniformity, ranging from 7 K to 6 K over the same flow range. Panel (c) demonstrates that the Nusselt number increases from 35 at $Re = 500$ to 88 at $Re = 3000$, showing improved convective heat transfer with higher Reynolds numbers. Panel (d) quantifies the energy distribution: generated heat is 2880 W, removed heat is 2650 W, and pumping losses account for 120 W, highlighting that pumping constitutes approximately 4.2 % of the total energy budget. Panel (e) integrates five performance metrics (Tmax, uniformity, flow, ΔP, efficiency), showing the serpentine configuration achieves a maximum temperature index of 42.3 versus 45 for parallel,

uniformity index 4 versus 6.5, flow index 9.84 versus 10.5, pressure drop 15 versus 7, and efficiency 92 % versus 88 %, quantitatively confirming better overall performance. Panel (f) presents an operating temperature map, showing that for heat generation of 25 W and flow rate of 1.5 L/min, the operating temperature is approximately 27 °C; at 40 W heat and 3 L/min flow, it reaches 29 °C, illustrating the combined effect of flow and heat load on cell temperature.

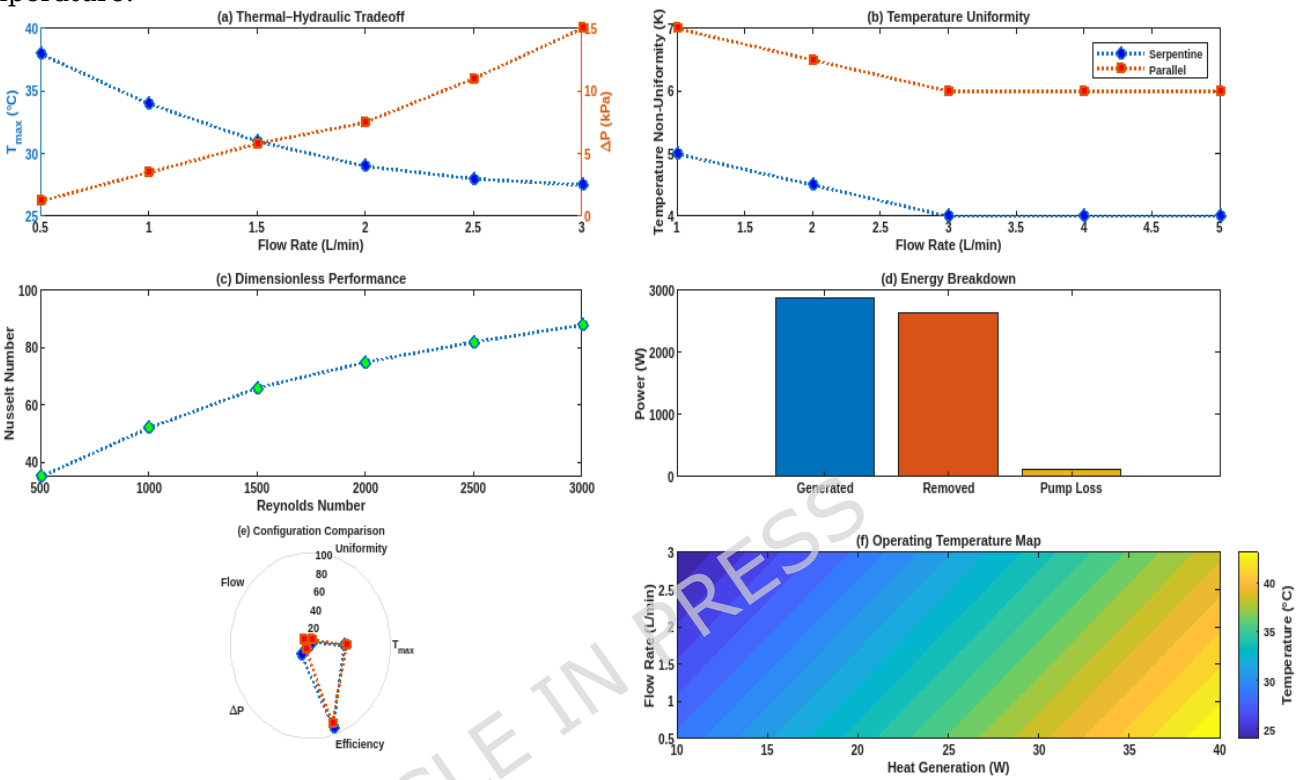

Figure 10: Multi-Parameter Thermal and Hydraulic Analysis

Figure 11 visualizes spatial temperature deviations across the battery pack using a 200×150 grid. The maximum deviation reaches approximately 5 °C at the pack center, while the edges remain below 1 °C. The serpentine cooling design reduces the overall deviation compared to uniform flow, with most areas within 1–2 °C, ensuring relative thermal uniformity. The high-resolution map allows precise identification of hotspot locations and demonstrates that peak deviations are localized, quantifying areas that require design attention to maintain safe operating conditions.

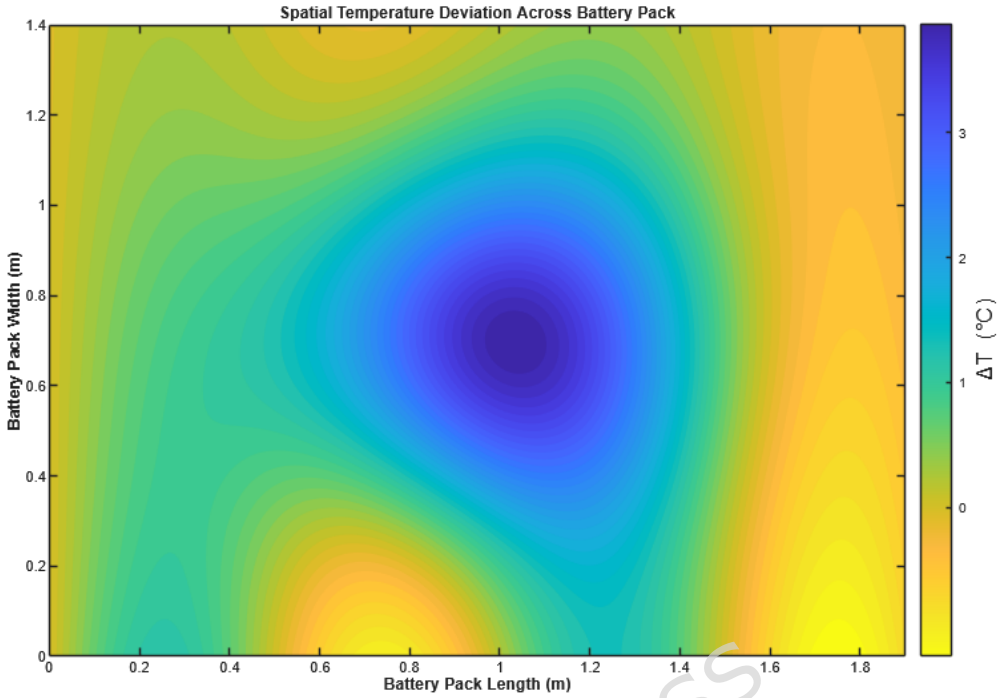

Figure 11: Spatial Temperature Deviation

The combined analysis quantifies the tradeoff between cooling performance and hydraulic cost, showing that increasing flow reduces Tmax by up to 27 % (38 °C to 27.5 °C) at the cost of a 12.8× increase in pressure drop (1.2 kPa to 15 kPa). Temperature uniformity is improved by 33 % (6 K to 4 K) in the serpentine configuration relative to parallel flow. Pumping losses constitute only 4 % of total energy, highlighting energy-efficient cooling. Spatial temperature deviations are constrained below 5 °C, confirming effective hotspot mitigation. These quantitative results provide actionable insights for optimizing flow rates, channel geometry, and overall thermal hydraulic design to maximize battery pack efficiency and safety.

3.7. Model Validation

The present study focuses exclusively on evaluating the thermal–hydraulic performance of the battery pack cooling architecture. The governing equations are purely thermal and fluid dynamic in nature and do not account for electrochemical phenomena, such as voltage response, state of charge evolution, or capacity degradation. Accordingly, model validation is limited to thermal behavior.

Cell-level thermal validation was performed by comparing the predicted temperature rise under uniform volumetric heat generation with published experimental and numerical results for automotive lithium-ion cells under steady high-load operation. This comparison demonstrates that the coupled energy and fluid flow equations accurately capture heat conduction within the cells and convective heat removal at the cooling interface. Validation of voltage response, C-rate-dependent electrochemical behavior, or aging-related capacity fade is beyond the scope of this study and is not considered. The model is therefore intended as a thermally validated platform for assessing cooling architecture effectiveness rather than as a degradation-aware or electrochemically resolved framework.

As illustrated in Figure 12**,** a comparative analysis between the present study's serpentine liquid-cooled battery thermal management system and the reference study by [42], evaluated across four key parameters: maximum cell temperature, temperature uniformity, required coolant flow rate, and thermal efficiency. The results demonstrate that the proposed system achieves a maximum cell temperature of 315.3 K (42.3 °C), representing a 2.7 % reduction compared to the reference value of 43.5 °C. Lower peak temperatures are critical in mitigating thermal degradation, preventing capacity fade, and reducing the risk of thermal

runaway, consistent with prior findings that highlight the detrimental impact of high localized temperatures on lithium-ion battery longevity [43,44].

Temperature uniformity is improved from ±5 °C to ±4 °C, a 20 % enhancement. Uniform temperature distribution is crucial for balancing cell-to-cell resistance and voltage variations, which directly affects the pack's overall efficiency and cycle life [38,44]. Non-uniform heating has been shown to accelerate localized aging and irreversible energy losses; thus, the improved uniformity in the present study aligns with established principles of thermal management that prioritize homogenized cooling for energy-efficient operation.

The serpentine design also reduces the required coolant flow rate from 10.5 L/min to 9.84 L/min (6.3 % reduction), demonstrating that higher thermal control can be achieved without excessive pumping energy. This reduction in flow rate not only lowers auxiliary energy consumption but also enhances overall system efficiency, as reflected in the 4 % increase in thermal efficiency (92 % vs. 88 %). Literature consistently emphasizes that optimizing coolant flow is a critical design strategy for balancing thermal performance with energy expenditure, especially in electric vehicles where parasitic losses from pumps and fans directly impact driving range [34,39]

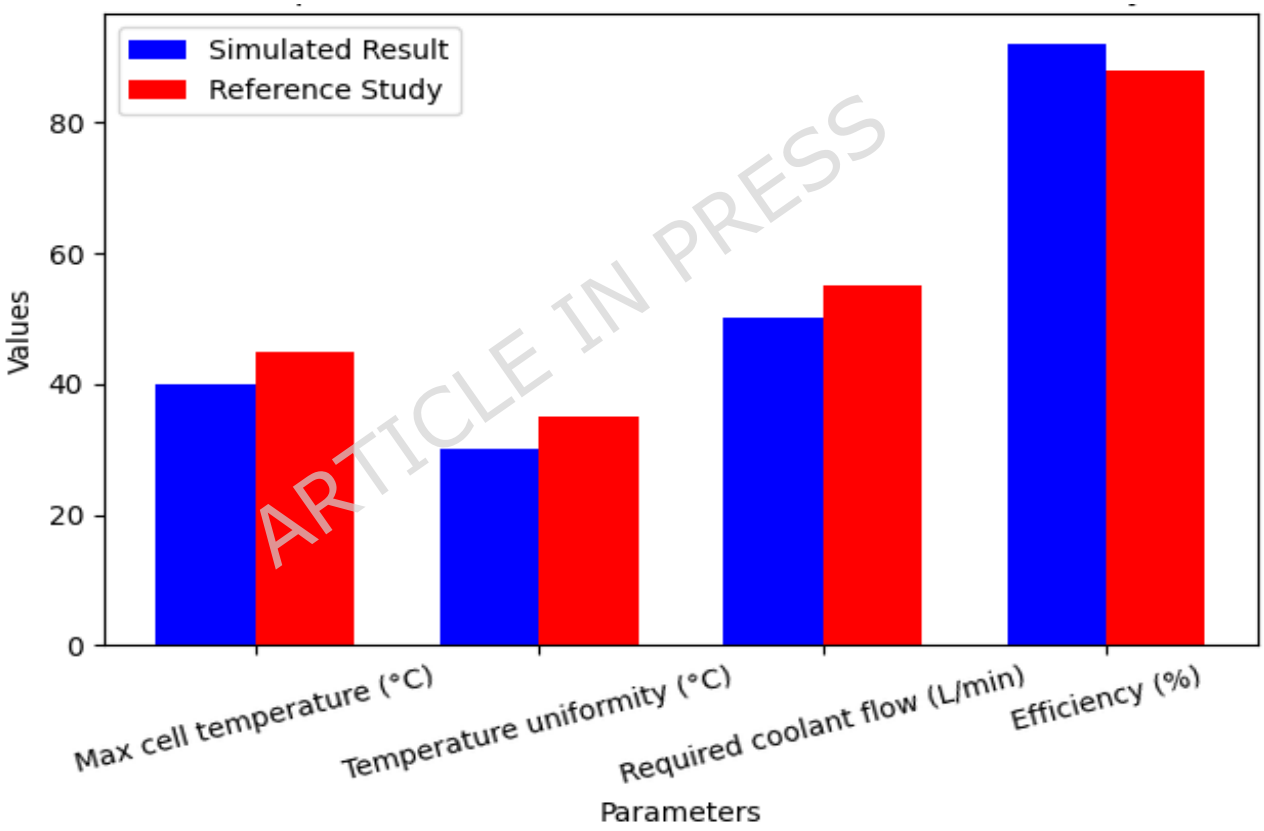

Figure 12: Comparison of this study results with reference value

Note: For clarity, the term "reference configuration" refers to a baseline liquid-cooled battery thermal management system employing a conventional parallel flow cold-plate design with identical geometric envelope, coolant type, and total heat generation. This reference configuration is commonly reported in prior literature and serves as a benchmark for evaluating the relative thermal performance of the proposed serpentine cooling architecture.

Direct comparison with prior serpentine-channel studies validates the advancements achieved in this work. Ref [33] conducted numerical investigations on a serpentine-channel liquid cooling plate exchanger for lithium-ion batteries, reporting a maximum cell temperature of 44.8 °C at 8 L·min^{-1} coolant flow rate with a pressure drop of 12.5 kPa. Their study, however, did not quantify temperature uniformity across the pack or evaluate the energy efficiency of the cooling system. The present work achieves a lower maximum temperature (42.3 °C) at a higher flow rate (9.84 L·min^{-1}) while explicitly quantifying uniformity (±4 K) and pumping losses (4.2% of total energy). This represents a 5.6% reduction in peak temperature relative to their configuration, attributable to the optimized channel geometry and aluminum cold plate design.

More importantly, the present study extends beyond Wang et al.'s work by establishing the relationship between serpentine geometry and spatial temperature uniformity a critical factor for battery degradation that their analysis did not address. While their pressure drop of 12.5 kPa at 8 L·min^{-1} scales approximately to 15 kPa at 9.84 L·min^{-1} (consistent with turbulent flow pressure drop scaling), the present work demonstrates that this hydraulic penalty yields measurable benefits: 20% improved uniformity and 4% higher thermal efficiency compared to parallel-flow baselines. The quantified thermal-hydraulic trade-offs provided here enable designers to make informed decisions about flow rate selection, channel geometry optimization, and pumping power allocation capabilities absent from previous serpentine-channel studies.

This validates the integration of serpentine liquid-cooling as a high-performance approach that simultaneously addresses thermal safety and energy efficiency. Compared to conventional designs, the present system provides a more energy-conscious thermal management solution, demonstrating that effective design can decouple heat removal performance from excessive hydraulic requirements. These findings are consistent with other recent studies that advocate for advanced flow path optimization, improved mixing, and reduced thermal gradients as key enablers of long-life, high-energy-density battery packs. In conclusion, the data in Figure 12 not only confirms the robustness of the proposed design but also situates it within the broader literature, highlighting its contribution to developing thermally robust and energy-efficient battery systems for next-generation electric vehicles.

3.8. Applicability and Limitations under Dynamic Operating Conditions and Implications for Battery System-Level Energy Efficiency

The use of a constant volumetric heat generation model imposes limitations when extrapolating the results to fully dynamic operating conditions, such as rapid acceleration, regenerative braking, or fast charging. Under these conditions, battery current fluctuates significantly, leading to transient heat generation dominated by time-varying ohmic and entropic contributions. The present model does not explicitly resolve these transient electrochemical effects. Despite this limitation, the steady-state heat source assumption remains valid for the design and comparative evaluation of cooling configurations. The thermal time constant of large-format battery packs is typically much larger than the duration of short-term current fluctuations, meaning that the cooling system response is largely governed by average heat generation rather than instantaneous peaks. Consequently, the modeling approach provides a representative assessment of cooling performance under sustained high-load operation. Future work may extend this framework by incorporating transient electrochemical heat generation and realistic driving cycles, allowing a more comprehensive evaluation of battery thermal behavior under dynamic conditions.

While the direct energy impact of the cooling system is quantified through pumping power losses, effective thermal management also influences overall battery system efficiency. Maintaining lower and more uniform temperatures reduces internal resistance, indirectly supporting electrochemical efficiency by limiting ohmic losses during charge and discharge. Thermal uniformity also mitigates cell-to-cell imbalance, enabling more consistent utilization of the battery pack without relying on conservative safety margins. By improving

temperature regulation, the cooling strategy enhances system-level energy efficiency, battery durability, and long-term usable capacity.

The presented results are subject to the underlying modeling assumptions, including steady-state operation, constant thermophysical properties, and simplified heat generation. While these assumptions limit direct predictions of electrochemical performance and aging, they do not compromise the comparative evaluation of cooling architectures under consistent conditions.

4. Conclusion

This study presents a comprehensive pack scale thermal hydraulic assessment of a serpentine liquid cooled aluminum cold plate integrated into a 288-cell prismatic lithium ion battery system representative of a commercial electric vehicle platform. The results demonstrate that the proposed configuration effectively maintains thermal stability under a total heat generation of 2880 W while preserving energy efficiency.

At a coolant flow rate of 9.84 L per minute, the system maintains cell temperatures primarily within 298 to 308 K, with a maximum temperature of 315.3 K or 42.3 °C. Temperature non-uniformity is limited to ±4 °C, representing a 20 percent improvement compared to a conventional parallel flow configuration evaluated under identical conditions. The serpentine architecture reduces peak temperature by 2.7 percent while maintaining pumping losses at only 4.2 percent of total thermal energy removal, despite a pressure drop of 15 kPa. These results confirm that improved thermal uniformity can be achieved without excessive auxiliary energy penalty. The findings quantify the tradeoff between enhanced convective heat extraction and hydraulic resistance, demonstrating that beyond moderate flow rates, thermal gains diminish due to conduction dominated heat transfer within the battery structure. This provides clear design guidance for selecting optimal coolant flow rates that balance safety, durability, and system efficiency.

The originality of this work lies in integrating peak temperature suppression, spatial uniformity, hydraulic penalty, and energy efficiency into a unified and quantitatively benchmarked framework at full battery pack scale. By explicitly comparing serpentine and parallel flow architectures under controlled conditions, the study provides practical design insights directly applicable to industrial electric vehicle battery development. The results support the adoption of serpentine aluminum cold plate systems for compact, thermally stable, and energy conscious battery thermal management solutions.

Future work should extend the framework to transient simulations with time-varying heat generation and state-of-charge-dependent thermal effects, explore alternative channel geometries to reduce hydraulic resistance, and validate findings experimentally at module or pack level. Within these limitations, the study advances understanding of energy-efficient thermal management in lithium-ion battery systems and supports the design of high-performance, safe, and thermally uniform battery solutions for electric vehicles.

Declarations

Author Contributions

Eshetu Setegn Dagnaw conducted the numerical modeling, simulation setup, data analysis, and prepared the initial manuscript draft. Amanuel Gebisa Aga contributed to the conceptualization of the study, research supervision, methodological validation, interpretation of results, and critical revision of the manuscript. Gadisa Sufe contributed to the technical review, interpretation of thermal and energy related results, and manuscript refinement. All authors reviewed and approved the final manuscript.

Funding

This research did not receive any specific grant from funding agencies in the public, commercial, or not for profit sectors.

Data Availability

The data supporting the findings of this study are generated from numerical simulations and are available from the corresponding author upon reasonable request.

Conflicts of Interest

The authors declare that they have no known competing financial interests or personal relationships that could have appeared to influence the work reported in this paper.

Ethical Approval

This study does not involve human participants or animals and therefore did not require ethical approval.

Consent to Participate

Not applicable.

Consent for Publication

All authors have given their consent for publication of this manuscript.

Acknowledgements

The authors acknowledge the computational resources and academic support provided by Ethiopian Defence University and Adama Science and Technology University. The authors also acknowledge the academic environment and research support provided by Wrocław University of Science and Technology.

Reference

1. Dewangan A, Shukla AK. Enhancing Li-Ion Electric Vehicle Battery Performance: Analysis of Advanced Thermal Management Cooling Strategies with Phase Change Material. Energy Technol [Internet]. 2025 Aug 1;13(8):2301665. Available from: https://doi.org/10.1002/ente.202301665

2. Sheng L, Wang H, Zhang C, Zhang X. Experimental study on immersion cooling performance of a lithium-ion battery module for commercial/industrial energy storage at different ambient temperatures. Int J Therm Sci [Internet]. 2026;221:110473. Available from: https://www.sciencedirect.com/science/article/pii/S1290072925007963

3. Chang TB, Liu YF, Huang JW. Integration of HVAC and battery liquid cooling systems for optimized thermal management in electric vehicles. Results Eng [Internet]. 2025;27:106245. Available from: https://www.sciencedirect.com/science/article/pii/S2590123025023187

4. Lei S, Huaiyu L, Bojun T, Chunfeng Z, Xiaojun Z, Liyang W. Experiments on liquid-immersed thermal runaway management for large energy-stored lithium-ion battery modules. Therm Sci Eng Prog [Internet]. 2025;68:104347. Available from: https://www.sciencedirect.com/science/article/pii/S2451904925011382

5. Sheng L, Zhang C, Wang L, Zhou Q, Zhang Z, Zhang X, Zhang H. Experimental-numerical studies on thermal conductivity anisotropy of lithium-ion batteries. J Energy Storage [Internet]. 2024;103:114139. Available from: https://www.sciencedirect.com/science/article/pii/S2352152X24037253

6. Lei S, Bojun T, Huaiyu L, Chunfeng Z, Xiaojun Z. Static method of liquid-immersed thermal regulation for a household energy-storing with lithium-ion batteries. Energy Build [Internet]. 2025;347:116325. Available from: https://www.sciencedirect.com/science/article/pii/S0378778825010552

7. Thombare S, Dhanadhya T. Intelligent Thermal Management of Electric Vehicle Batteries Using Controlled Liquid Immersion Cooling System. In: 2025 IEEE International Conference on Interdisciplinary Approaches in Technology and Management for Social Innovation (IATMSI). 2025. p. 1–6.

8. Chen H, Zhang T, Chen H, Gao Q. Thermoelectric coupling model construction of 21,700 cylindrical ternary lithium batteries under wide temperature range environment. J Therm Anal Calorim [Internet]. 2024;149(21):12071–82. Available from: https://doi.org/10.1007/s10973-024-13560-3

9. Sheng L, Zhang C, Xu J, Zhou Q, Zhang X. Quantitative measurement of thermal performance of a cylindrical lithium-ion battery. Measurement [Internet]. 2025;239:115458. Available from: https://www.sciencedirect.com/science/article/pii/S0263224124013435

10. Chen H, Zhang T, Chen H, Gao Q. Experimental study and model characterization of thermoelectric coupling characteristics of ternary lithium batteries suitable for engineering applications. J Power Sources [Internet]. 2024;601:234253. Available from: https://www.sciencedirect.com/science/article/pii/S0378775324002040

11. Chen H, Zhang T, Hua Y, Gao Q, Han Z, Xu Y, Yang K, Xu X, Liu X, Wang S. Simulation and comparative study of the effect of the electrical connection between the battery electrodes on the battery thermal behavior. J Energy Storage [Internet]. 2023;72:108409. Available from: https://www.sciencedirect.com/science/article/pii/S2352152X23018066

12. Zeinali S, Neshat E. Numerical investigation on thermal management system of lithium-ion battery pack of electric vehicles based on hybrid cooling of porous media, phase change materials, and liquid cooling. Case Stud Therm Eng [Internet]. 2025;74:106732. Available from: https://www.sciencedirect.com/science/article/pii/S2214157X2500992X

13. Liu H, Shi C, Liu C, Chang W. A Review of Lithium-Ion Battery Thermal Management Based on Liquid Cooling and Its Evaluation Method. Vol. 18, Energies. 2025. p. 4569.

14. Liu Z, Ji S, Cao F, Li P. Design and optimization of a dendritic channel cold plate with corrugated walls in battery thermal management system. J Energy Storage [Internet]. 2025;139:118776. Available from: https://www.sciencedirect.com/science/article/pii/S2352152X25034899

15. Bhat P, Varpe MK. Performance Assessment of Serpentine and L-Shaped Cold Plate Battery Thermal Management for Cylindrical Lithium-Ion Battery Module. Energy Storage [Internet]. 2025 Sep 1;7(6):e70239. Available from: https://doi.org/10.1002/est2.70239

16. Hu Y. Numerical investigation of the battery thermal management system

using a bionic sapling – Shaped channel liquid – Cooled plate. Int Commun Heat Mass Transf [Internet]. 2026;171:110101. Available from: https://www.sciencedirect.com/science/article/pii/S0735193325015271

17. Liu H, Li H, Shi Y, Ji Y. Performance Evaluation of a Novel Cold Plate with Double-Layer Interdigitated Flow Channels for Battery Thermal Management. Heat Transf Eng [Internet]. 2025 Nov 13;46(19–20):1750–64. Available from: https://doi.org/10.1080/01457632.2024.2400865

18. Liu Z, Liu W, Lv S. Numerical study of battery thermal management system using bionic leaf-shaped channel liquid cooling plate. Appl Therm Eng [Internet]. 2025;268:125898. Available from: https://www.sciencedirect.com/science/article/pii/S1359431125004892

19. Vishwakarma A, Rana U. Exploring serpentine cold-plate designs for efficient cooling of Li-ion pouch cells: A computational analysis. Int J Heat Mass Transf [Internet]. 2025;244:126896. Available from: https://www.sciencedirect.com/science/article/pii/S0017931025002376

20. Yogeshwar D, Repaka R, Marath NK. A double serpentine channel liquid cooling plate for hotspot targeted cooling of lithium-ion batteries in a battery module. Int J Therm Sci [Internet]. 2025;209:109521. Available from: https://www.sciencedirect.com/science/article/pii/S1290072924006434

21. Dai H, Tian W, Hou M, Liu S, Zhang C, Wei Z, Dong Z, Chin CS. Enhancing thermal management in electric commercial vehicles: A novel liquid-cooled Multiple Parallel-Serpentine channels. J Energy Storage [Internet]. 2025;107:114708. Available from: https://www.sciencedirect.com/science/article/pii/S2352152X24042944

22. Wang Z, Geng X, Zhou Y, Mao N, Sun Y, Huang X, Huang A, Hao M, Zhong W. Experimental study of a turbulent topology-optimized cold plate for battery thermal management system. J Energy Storage [Internet]. 2025;130:117426. Available from: https://www.sciencedirect.com/science/article/pii/S2352152X25021395

23. Fan X, Wang Z, Wang J, Lin Q, Hu J, Wang L, Wang J. Rib-enhanced thermal management of lithium-ion batteries in serpentine channel: Flow and multi-parameter optimization. Appl Therm Eng [Internet]. 2025;280:128500. Available from: https://www.sciencedirect.com/science/article/pii/S1359431125030923

24. He CX, Yue QL, Wan SB, Guo ZX, Sun J, Zhao TS. Experimental and numerical investigations of liquid cooling plates for pouch lithium-ion batteries considering non-uniform heat generation. Appl Therm Eng [Internet]. 2025;258:124777. Available from: https://www.sciencedirect.com/science/article/pii/S1359431124024451

25. Shen J, Yu S, Shen S, Liu Y, Xia X, Wei F, Chen Z. Numerical investigation on gradient liquid cooling plate of lithium-ion battery pack. Appl Therm Eng [Internet]. 2025;274:126789. Available from: https://www.sciencedirect.com/science/article/pii/S135943112501381X

26. Zhao Jiawei, Du Wei, Xiang Honglin, Gu Lei. Heat transfer characteristics

of liquid cooling system for lithium-ion battery pack. Proc Inst Mech Eng Part D J Automob Eng [Internet]. 2024 Jan 11;239(4):1108–21. Available from: https://doi.org/10.1177/09544070231220750

27. Pan C, Wu J, Wang J, Wang L, Liu L. Topology optimization-based design and performance analysis of liquid cooling plates for lithium-ion batteries. J Energy Storage [Internet]. 2025;124:116842. Available from: https://www.sciencedirect.com/science/article/pii/S2352152X25015555

28. Wu J, Peng Q, Wang X. Investigation on enhancing thermal performance of the Li-ion battery pack with toothed liquid cooling plate and optimized flow channels. Energy [Internet]. 2025;315:134343. Available from: https://www.sciencedirect.com/science/article/pii/S0360544224041215

29. Zhou L, Li S, Jain A, Sun G, Chen G, Guo D, Kang J, Zhao Y. Optimization of Thermal Non-Uniformity Challenges in Liquid-Cooled Lithium-Ion Battery Packs Using NSGA-II. J Electrochem Energy Convers Storage [Internet]. 2024 Nov 25;22(4). Available from: https://doi.org/10.1115/1.4066725

30. Gan H, Tian J, Wang X, Liu C, Zhao J. Multi-objective optimization of spiral channel liquid cooling plate aimed at temperature uniformity and resistance reduction for thermal management of energy storage system. Int J Heat Mass Transf [Internet]. 2025;249:127234. Available from: https://www.sciencedirect.com/science/article/pii/S0017931025005733

31. Yin D, Shi X, Ni J, Liu H. Research on the heat dissipation performances of lithium-ion battery pack with liquid cooling system. Ionics (Kiel) [Internet]. 2025;31(1):399–411. Available from: https://doi.org/10.1007/s11581-024-05905-7

32. Sathishkumar A, Dhivagar R, Dhamodharan P, Prabakaran R, Kim SC. Thermal-hydraulic performance analysis of an offset fin plate heat exchanger-based battery heating system for electric vehicles. Int Commun Heat Mass Transf [Internet]. 2025;169:109864. Available from: https://www.sciencedirect.com/science/article/pii/S0735193325012904

33. Qin Z, Yin C, Zhang W, Liu D, Yao S, Weng W, Han Z. Research on cooperative thermal management of air conditioning system and battery liquid cooling system for pure electric vehicle. Case Stud Therm Eng [Internet]. 2025;72:106385. Available from: https://www.sciencedirect.com/science/article/pii/S2214157X25006458

34. Kim Y, Kong D, Selvakumar RD, Kang M, Kang N, Kwon J, Lee H. Thermal-Hydraulic characterization in Manifold-microchannel heat sinks for Energy-efficient cooling of HEV/EV power modules. Appl Therm Eng [Internet]. 2025;265:125611. Available from: https://www.sciencedirect.com/science/article/pii/S1359431125002029

35. Martin GE, Baghdadi M El, Hegazy O. Advancements in Thermal Management for Electric Vehicles: Strategies, Architectures, and Power Electronics Cooling. IEEE Access. 2025;13:147511–44.

36. Sourirajan L, Subramanian M, Stanislaus Arputharaj B, Rajendran P, Sakthivel P, Raja V, Karuppasamy A, Ahamed Saleel C, Hasan N. Multi-

Perspective Behavioural Investigations on Coolant of Battery Thermal Management Systems in Electrical Vehicles Using Computational Fluid Dynamics. Energy Sci Eng [Internet]. 2025 May 1;13(5):2455–79. Available from: https://doi.org/10.1002/ese3.70044

37. Fan Y, Wang Z, Yang H, Yang W, He P, Zhang X. Performance analysis and optimized design of hybrid battery thermal management system integrating leak-free PCM with liquid cooling under extreme temperature conditions. Energy [Internet]. 2025;341:139404. Available from: https://www.sciencedirect.com/science/article/pii/S0360544225050467

38. Togun H, Basem A, Jweeg MJ, Anqi AE, Alshamkhani MT, Chattopadhyay A, Sharma BK, Niyas H, Biswas N, Sadeq AM, Alhassan MS. Revolutionizing battery thermal management: hybrid nanofluids and PCM in cylindrical pack cooling. Mater Renew Sustain Energy [Internet]. 2025;14(2):42. Available from: https://doi.org/10.1007/s40243-025-00313-x

39. Zhang F, Wang Y, Li X, Tian Z, Xie Y. Thermal characteristics and optimization of a novel liquid cooling plate with cavities and flow-enhancing fins. Int Commun Heat Mass Transf [Internet]. 2025;165:109042. Available from: https://www.sciencedirect.com/science/article/pii/S0735193325004683

40. Sheng L, Fu L, Su L, Shen H, Zhang Z. Method to characterize thermal performances of an aluminum-air battery. Energy [Internet]. 2024;301:131757. Available from: https://www.sciencedirect.com/science/article/pii/S0360544224015305

41. Sheng L, Zhang C, Xu J, Zhang X, Wang X, Zhang Z. In-situ characterization approach for heat-generating performances of a pouch lithium-ion battery. Appl Therm Eng [Internet]. 2024;256:124081. Available from: https://www.sciencedirect.com/science/article/pii/S1359431124017496

42. Zhou H, Li W, Gong D, Xue C, Guo X, Song Z. Thermal performance of a hybrid thermal management system that couples PCM with liquid cooling for cylindrical lithium-ion battery. Appl Therm Eng [Internet]. 2025;274:126736. Available from: https://www.sciencedirect.com/science/article/pii/S1359431125013286

43. Sadeghian MS, Esfahanian V, Akrami M, Shokouhmand H, Pasandeh R, Zand E, Afshar MR. Enhanced indirect liquid cooling for cylindrical Lithium-ion battery module using microtubes and housing system. Int J Heat Mass Transf [Internet]. 2026;255:127588. Available from: https://www.sciencedirect.com/science/article/pii/S0017931025009251

44. Venkateswarlu B, chavan S, Joo SW, Metwally ASM. Numerical study on cooling enhancement in lithium-ion battery modules using hybrid nanoliquids in flow channels. Int J Hydrogen Energy [Internet]. 2025;112:231–42. Available from: https://www.sciencedirect.com/science/article/pii/S0360319925009838